HEAT TRANSFER FROM MOLTEN

MATERIALS TO LIQUIDS.

A thesis submitted for the degree of

PhD

by GAREPH BOXLEY

at The University of Aston in Birmingham

in September, 1980.

Summary

An apparatus was designed and constructed which enabled material to be melted and heated to a maximum temperature of 1000°C and then flooded with a pre-heated liquid.

A series of experiments to investigate the thermal interaction between molten metals (aluminium, lead and tin) and sub-cooled water were conducted. The cooling rates of the molten materials under conditions of flooding were measured with a high speed thermocouple and recorded with a transient recorder.

A simplified model for calculating heat fluxes and metal surface temperatures was developed and used.

Experimental results yielded boiling heat transfer in the transition film and stable film regions of the classic boiling curve. Maximum and minimum heat fluxes were observed at nucleate boiling crisis and the Leidenfrost point respectively.

Results indicate that heat transfer from molten metals to sub-cooled water is a function of temperature and coolant depth and not a direct function of the physical properties of the metals.

Heat transfer in the unstable transition film boiling region suggests that boiling dynamics in this region where a stationary molten metal is under pool boiling conditions at atmospheric pressure would not initiate a fuel-coolant interaction. Low heat fluxes around the Leidenfrost point would provide efficient fuel-coolant decoupling by a stable vapour blanket to enable coarse mixing of the fuel and coolant to occur without appreciable loss of thermal energy from the fuel.

The research was conducted by Gareph Boxley and was submitted for the degree of PhD at the University of Aston in Birmingham in 1980.

Index: Heat Transfer Molten Metals/Water.

This thesis 'Heat transfer from Molten Materials to Liquids' is an account of the study done under the supervision of Professor F.M. Page., BA., PhD., ScD., at the University of Aston in Birmingham, during the period November 1976 to August 1979.

The work described is original, except where stated, and has not been, or is being, submitted for any other degree or award.

September 1980 G.Boxley.

Acknowledgments

The author wishes to gratefully acknowledge the help, guidance and encouragement given to him by his supervisor Professor F.M. Page, and by his associate supervisor Professor W.O.Alexander. He would also like to extend his thanks to Hazel Whiting for graciously typing the manuscript and to Fiona Kendrick and Justin Kendrick for their constructive criticism and proof reading of the manuscript.

Financial support was gratefully received from the Health and Safety Executive.

C O N T E N T S .

List of Tables

List of Figures

Chapter I

Introduction

Considerable interest has been generated in recent years concerning the explosive vaporisation of a cold liquid which may occur when it is brought into contact with another liquid at a higher temperature. Frequently the terms 'fuel' and 'coolant' are used as nomens for the hot and cold liquids respectively and the phenomenon referred to as a fuel-coolant interaction (F.C.I.). The phenomenon is also called a vapour explosion or a physical explosion, indicating that the interaction is not the release of chemical energy but involves the physical transfer of the stored thermal energy of the fuel, to the coolant.

Epstein (1) has shown that for a metal/water interaction, every water molecule in contact with the metal surface would have to react in order to produce the energy that has been observed in such interactions, and that such an occurrence would be extremely unlikely. Witte and Cox (2) have considered the physical process of heat transfer and have concluded that the observed energy transfer is of the order of 10^3 above that observed in normal boiling heat transfer processes.

Comminuation of the fuel to increase the surface area of contact would facilitate greater heat fluxes, and Dullforce, Buchanan and Peckover (3), Page et al (4) have examined the solid fuel after interaction and have found fine fragmented debris ranging in size from a few microns to a few millimetres. Metal/water

contact resulting in partial interaction, Page et al (5), results in macro debris with an interesting cellular structure. F.C.I. phenomenon is not restricted to molten metal/water systems, and can occur between a wide range of liquid combinations, providing that there is sufficient thermal energy, and that the coolant is volatile. Furthermore such interactions are of historic note and a pamphlet in the Ironbridge Museum (6) records the destruction of the Old Furnace at Coalbrookdale in 1801 when it was reported to have been flooded following a rainstorm. Many instances have been reported since then, Morrison (7) for example quotes the case in the mid 1870's when a careless workman dropped molten steel into a pit of water while a U.S. Senator was inspecting the improved Bessemer process for steel making. The force of the explosion threw the Senator across the shop. Probably the largest example of a F.C.I. was the destruction of Krakatoa, Macdonald (8) in 1883 with an estimated explosive yield equivalent to 200M tons of TNT. More recently, F.C.I.'s have been reported in a wide range of industries which include the Chemical; Oil and Natural Gas; Pulp and Paper; Metal Foundry; and Nuclear Reactor Industries.

In the Chemical Industry Jennings (9) quotes several examples where hot and cold liquids become intermixed with disastrous results. For instance the filling of a road tanker with hot tar at 150^{o}C the tanker contained water and a few seconds after filling commenced the tank erupted due to the interaction of

hot tar and water. Another example quoted, concerned a light oil which contained small quantities of water. The oil was heated to drive off the water vapour prior to carrying out a reaction. Heating was started without agitation and it was assumed that the stratification of the oil and water resulted in the oil being heated to above the boiling point of water, the heating coils were estimated to be at 250°C. Agitation was finally started but this forcibly mixed the hot oil and relatively cold water together resulting in a vapour explosion.

King (10) has suggested that the Flixborough disaster was initiated by a F.C.I. in one of the reactor vessels when the stirrer was turned on, mixing hot cyclohexane and water. The resulting pressurisation was sufficient to burst a temporary connection between two of the reactor vessels allowing cyclohexane to escape. The damage was then caused by the subsequent explosion of the cyclohexane/air cloud.

While there have not been many incidents in the Oil and Natural Gas Industries, Hughes (11) has reported several incidents where large heavy oil storage tanks have been destroyed by the sudden vaporisation of water which had become trapped in the hot oil. While with natural gas the U.S. Bureau of Mines (12) reported vapour explosions when investigating the effects of large scale spillage of liquid natural gas (LNG) onto water. Here the water was acting as the fuel and the liquid gas as the volatile coolant.

The Pulp and Paper Industry has a long history of industrial accidents in the soda recovery operation of the pulp making process which can be attributed to the F.C.I. phenomenon. Nelson and Kennedy (13) and (14) have investigated incidents of smelt dropping into the green-liquor and concluded that such explosions were physical and not chemical in nature, and in 1962 as a result of the increased frequency and severity of recovery boiler explosions the Black Liquor Recovery Boiler Advisory Committee was set up. Taylor and Gardner (15) have reviewed some 59 accidents resulting from smelt/water explosions between 1948 and 1973.

Explosive incidents resulting from the accidental contact of metal and water have occurred for many years in the metal foundry industry. The major incidents have been reviewed by Vaughan (16) and Buxton and Nelson (17). The most recent major incident in the U.K. occurred at Scunthorpe in 1975 (18). The accident occurred at the British Steel Corporation's plant at Appleby - Frodingham Steelworks, and a total of 11 people were killed and 8 injured. The incident occurred because of the failure of a blast furnace cooling pipe and the water found its way into an insulated rail torpedo containing some 175 to 200 tons of molten steel. When the torpedo was attached to a locomotive to move it,an explosion occurred. It was not certain what action, if any, of the locomotive initiated the incident. Estimates of the amount of water involved were between 400 to 700 gallons.

The F.C.I. phenomenon is of interest to the nuclear reactor industry and incidents have occurred with small water cooled research reactors. The danger exists that during a power surge the water filled metal heat exchangers could melt resulting in the mixing of molten metal and water, and/or molten core material. Such an explosion would severely damage the reactor and may result in a scenario of a catastrophic nature.

In general there appear to be three factors necessary for a F.C.I. to occur these are; that the fuel or hot material is molten; that the interface temperature between the fuel and coolant is at least that of the superheat limit of the coolant; and that heat transfer is initially by stable film boiling.

When the hot material is in liquid phase then it is possible that its surface area can be greatly increased over a short time scale thus enabling rapid heat transfer to occur. With a solid phase fuel such rapid fragmentation is thought not to be possible, though some materials for example UO_2 will fragment due to thermal stressing but such fragmentation is relatively slow.

The interface temperature Ti is derived from the instantaneous contact temperature of two semi infinite solid materials and is given by Carslaw and Jaeger (19) as

$$Ti = \frac{\alpha_F T_F + \alpha_C T_C}{\alpha_F + \alpha_C} \qquad \ldots (1.01)$$

Where T is the initial temperature

α is $(Kpc)^{\frac{1}{2}}$

K is the thermal conductivity

C is the specific heat

ρ is the density

and subscripts F and C refer to fuel and coolant respectively. The superheat factor is based upon the belief, for example Fauske (20) that spontaneously triggered F.C.I.'s cannot occur if the interface temperature Ti is below the spontaneous nucleation temperature of the coolant, and that the coolant is raised on contact with the fuel to its superheat limit. At this point there is an instantaneous phase change in the coolant, and the associated pressure pulse of the vapour formation is assumed to initiate a local interaction.

The third factor, that of stable film boiling, enables the separation of fuel and coolant to occur and thus facilitates coarse mixing with reduced loss of thermal energy due to the low heat flux associated with stable film boiling. For film boiling to occur Ti must be equal to or above the minimum temperature to sustain stable film boiling. For the above three factors to occur in a typical commercial environment for molten metal/water interactions then boiling heat transfer would occur.

Chapter II

Boiling Heat Transfer and Pool Boiling

Boiling heat transfer is defined by Tong (21), as a mode of heat transfer that occurs with a change in phase from liquid to vapour. The existence of several regimes of boiling was first clearly discussed by Nukiyama (22), although Leidenfrost (23) and Lang (24) had reported the existence of minimum and maximum rates of boiling heat transfer. Later the experiments in pool boiling with an electrically heated horizontal wire submerged in a tank of saturated water reported by Farber and Scorah (25) and McAdams et al (26) again verified the boiling regimes suggested by Nukiyama (22).

Consider Fig (2.01) page 8, which is the conventional log-log representation of heat flux versus wall superheat.

In region I free-convection currents are responsible for the motion of the fluid near the surface. In this region the liquid near the heated surface is superheated slightly, and it subsequently evaporates when it rises to the surface. In region II bubbles begin to form on the surface of the wire and are dissipated in the liquid after breaking away from the surface. This is known as local boiling, that is the bulk of the liquid is subcooled. The region indicates the beginning of nucleate boiling and the bulk temperature is increased, further vapour bubbles form more rapidly and rise to the surface of the liquid where they are dissipated and bulk boiling is said to occur. This is indicated in region III, where a small change in

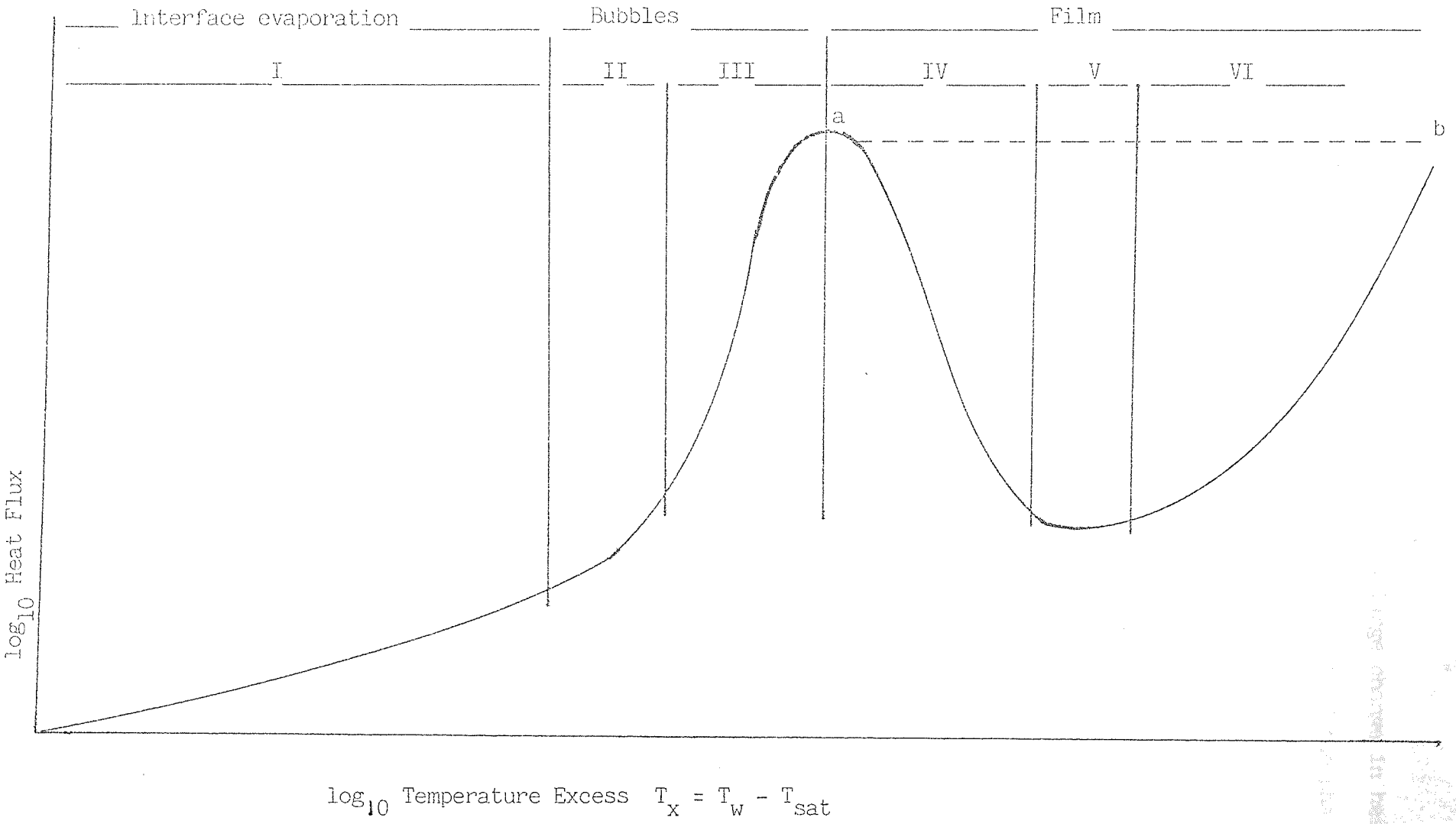

Figure 2.01 Heat-Flux data From Farber and Scorah (25)

temperature excess is associated with a large change in heat flux. Vapour bubbles transport the latent heat of the phase change and also increase the convective heat transfer by agitating the liquid near the heating surface.

Maximum nucleate boiling heat transfer occurs at point 'a' which is known as the boiling crisis or burn-out or D.N.B. (Departure from Nucleate Boiling). It is caused by the rapid formation of vapour bubbles which obstruct the inflow of fresh liquid and at this point the vapour bubbles coalesce and form a vapour film which covers the surface. Heat must be conducted through this film before it can reach the liquid and effect the boiling process. The thermal resistance of this film causes a reduction in heat flux, and this phenomenon is illustrated in region IV, the transition film boiling region. This region represents a transition from nucleate boiling to film boiling and is unstable. Stable film boiling is eventually encountered in region V which represents a minimum heat transfer region where a large change in temperature excess is associated with this minimum heat flux and is known as the Leidenfrost temperature. The surface temperatures required to maintain stable film boiling are high, and once this condition is attained, a significant portion of the heat lost by the surface may be the result of thermal radiation, as indicated in region VI. In many practical situations the temperature necessary to maintain high heat fluxes in region VI results in damage to the heater, and the heater may melt before point 'b' on the boiling curve is reached.

Pool boiling is the type of boiling that occurs when a heater is submerged in a pool of initially stagnant liquid. When the surface temperature of the heater sufficiently exceeds the saturation temperature of the liquid, vapour bubbles nucleate on the heater surface. The bubbles grow rapidly in the superheated liquid layer next to the surface until they depart and move out into the bulk liquid. While rising as the result of buoyancy they either collapse or continue their growth, depending upon whether the liquid is locally subcooled or saturated. Thus in pool boiling a complex fluid motion around the heater is initiated and maintained by the nucleation growth, departure, and collapse of bubbles and by natural convection.

The rate of heat transfer in nucleate pool boiling is usually very high and Forster and Greif (27) attribute this high flux to microconvection in the superheated liquid sublayer adjacent to the heater surface. This motion is caused by the dynamics of bubbles that nucleate and grow in the superheated film. As the bubbles are strong agitators and the heat flux appears to be independent of the geometry of the system and insensitive to the degree of liquid subcooling, increased subcooling reduces bubble size and thus reduces the intensity of agitation, but this effect is nearly cancelled by subcooling effect on turbulent liquid convection.

Vapour bubble nucleation and hydrodynamics has been the subject of much research and Cole (28) gives a good review of the subject.

In brief the life of the single bubble may be summarized as occurring in the following phases:

nucleation

initial growth

intermediate growth

asymptotic growth

possible collapse

Nucleation is a process, on a molecular scale, in which a bubble nucleus of size just in excess of the thermodynamic equilibrium is formed. Initial growth from the nucleation size is controlled by inertia and surface tension effects. The growth rate is small at first but increases with bubble size as the surface tension effects become less significant. In the intermediate stage of accelerated growth, heat transfer becomes increasingly important, while inertia effects begin to lose significance. When the growth process reaches the asymptotic stage, it is controlled by the rate of heat transferred from the surrounding liquid to facilitate the evaporation at the bubble interface. If the bubble, during its growth contacts subcooled liquid it may collapse. The controlling phenomenon for the collapse process are much the same as for the growth process but are encountered in reverse order.

Consider a spherical bubble in a liquid, the pressure force of the liquid and vapour must be balanced by the surface tension force at the vapour-liquid interface. The pressure force acts

on an area of πr^2 , and the surface tension acts on the interface length of $2 \pi r$. The force balance is:

(2.01)

$$\pi r^2 (p_v - p_l) = 2 \pi \sigma r$$

or $$p_v - p_l = \frac{2\sigma}{r}$$

where p_v is the vapour pressure inside the bubble

p_l is the liquid pressure

σ is the surface tension of the vapour-liquid interface.

Equation (2.01) indicates that as $r \rightarrow o$, $p_v - p \rightarrow \infty$ and implies that a vapour bubble can never be created. However nucleation can occur due to cavities on the heater surface or suspended foreign material or entrained gas. Nucleation occurs in such cases with a heater wall superheat only marginally in excess of the saturation temperature of the liquid.

In the absence of nucleation sites a metastable superheated liquid develops. Nucleation in such a liquid can take place in two forms called homogeneous nucleation and heterogeneous nucleation.

Homogeneous Nucleation

Homogeneous nucleation is the nucleation in superheated liquid due to internal molecular density variation and by definition represents the maximum superheat attainable. The theory of homogeneous nucleation has been developed from the early ideas of Becker and Döring (29), Volmer (30) and Frenkel (31)who

who have emphasized the kinetic approach. More recently, statistical-mechanical concepts have been put forward by Reiss (32), Lothe and Pound (33) and Reiss, Katz and Cohen (34). The subject has been reviewed by Hirth and Pound (35)and Zettlemoyer (36).

The Kinetic approach assumes that the liquid is composed of molecules which are considered to have a distribution of energies such that only a small fraction have energies considerably greater than the average. Such 'activated' molecules, their excess energy being called the'energy of activation' are presumed to initiate the formation of vapour bubbles. As a probability of a sufficient number of such highly activated molecules being in the same region of space at the same time is negligibly small, the nucleation process is considered to occur by a step-wise reversible collision process.

It can be shown that the maximum free energy of formation is:

(2.02)

$$E_f = \frac{4 \pi \sigma r^{*2}}{3}$$

Where r^* is the critical radius of the bubble.

Now the number of nuclei of radius r which may form in a liquid with c molecules per unit volume is:

(2.03)

$$N_r = c. \exp\left(\frac{-\Delta G (r)}{k T}\right)$$

Where k is the Boltzman constant.

Such nuclei will grow if they have the equilibrium radius for the temperature of the liquid and their size is increased by the collision of further molecules with sufficient energy so as not to deactivate the cluster.

The probability of such a collision has been given by Westwater (37) and Bernath (38) as

$$\text{Probability} = \frac{kT}{h} \quad \text{and}$$

$$\text{Probability} = \left(\frac{2\sigma}{\pi m}\right)^{\frac{1}{2}} \quad \text{respectively.}$$

Hence:

$$N_r = C.\ \text{Probability}.\ \exp\left(\frac{-4h\sigma r^{*2}}{3\,kT}\right) \qquad (2.04)$$

Where h = Planck's constant

and m = the mass of one molecule

The transcendental equation has been solved for given values of N_r by Enger and Hartman (39) for a variety of liquids, and they have compared them to experimental values from Apfel (40).

Cole (28), using Westerwater's (37) probability factor and settling N_r = one nucleation site per cubic centimetre per second has obtained an approximate expression for the superheat limit.

(2.05)

$$T_L - T_{sat} = \frac{T_{sat}}{P_v L_v} \left(\frac{16 \pi \sigma^3}{3 k \quad T_L \quad L_v \ln\left(\frac{ck\ T_L}{h}\right)} \right)^{\frac{1}{2}}$$

Where T_L is the liquid temperature

T_{sat} is the saturation temperature

L_v is the latent heat of evaporation

k is Boltzmans constant

C is the number of molecules per unit volume

σ is the surface tension

h is Plank's constant.

This yields the maximum superheat for water to be 166°C which is in good agreement with the experimental value of 170°C of Kenrick et al (41), and 164°C of Briggs (42).

Heterogeneous Nucleation

Superheats predicted by homogeneous nucleation theory are typically an order of magnitude greater than those occurring in many engineering systems. Since in such systems nucleation is observed to occur on the bounding surfaces rather than in the bulk of the liquid, the solid surface must contain preferred

nucleation sites. It is generally held that such solid surfaces contain surface asperities which due to entrapped gas act as nucleation sites and so limit obtainable superheats. Bankoff (43) has considered the case of a liquid spreading over a surface containing grooves and cavities. It would be expected that over extended periods of time and through many thermal cycles at the heat transfer surface that the noncondensible component of entrapped gas in surface asperities would be replaced by vapour. Hence nucleation from such sites would commence at a negligibly small superheat which would then increase to some maximum stable value as the noncondensible component is swept out by dilution. Bankoff (44) indicates that this has been experimentally observed.

At a liquid-liquid interface the above type of nucleation site does not exist and therefore nucleation at the interface depends upon the strength of adhesion between the two surfaces. If the surface bonding strength is high, nucleation will take place in the relatively cooler bulk of the cold liquid, despite the temperature gradient of the liquid giving a higher tempenature at the interface, this being especially so when the cold liquid contains suspended foreign bodies or entrained gas. However, if the two liquids do not 'wet' each other then the bonding at the interface will be weak, and when heated, the bonds will break and cause nucleation at the interface. This will be

at a temperature below the theoretical superheat limit, that is the homogeneous nucleation temperature of the coolant.

Cole (28) in a development of Volmer (30), Fisher (45) and Bankoff (46) has shown that the superheat limit can be calculated using the expression

$$T_L - S_{sat} = \frac{Tsat}{p_v L_v} \left(\frac{16 \pi \sigma^3 f(\theta)}{3K T_L Ln\left(\frac{ckT_L}{h}\right)} \right)^{\frac{1}{2}} \qquad (2.06)$$

Where the nomenclature is the same as equation (2.05) but $f(\theta)$ is a function of the contact angle.

$$f(\theta) = \frac{1}{4}(2+3\,Cos\,\theta - Cos^3\theta) \qquad (2.07)$$

Where θ is the angle indicated in figure. 2.01 below

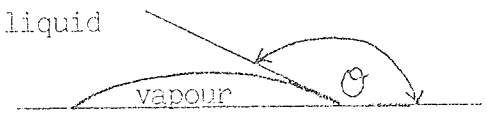

The derivation of equation (2.06) assumes the vapour embryo to be a portion of a sphere. For $\theta = 0$ the liquid completely wets the surface $f(\theta) = 1$, thus the heterogeneous superheat is the same as the homogeneous superheat. A value of $\theta = 180^\circ$ yields $f(\theta) = 0$ and presumably no superheat is attainable. However according to Bankoff (46) such a contact angle has not been recorded. For $\theta = 90^\circ$ $f(\theta) = 0.5$ and the superheat

is reduced by approximately 30%.

Vapour bubble formation at the interface between two immiscible liquids has been considered by Apfel (47), who has derived an expression for the effective surface tension which exists in such a situation as illustrated in figure (2.02).

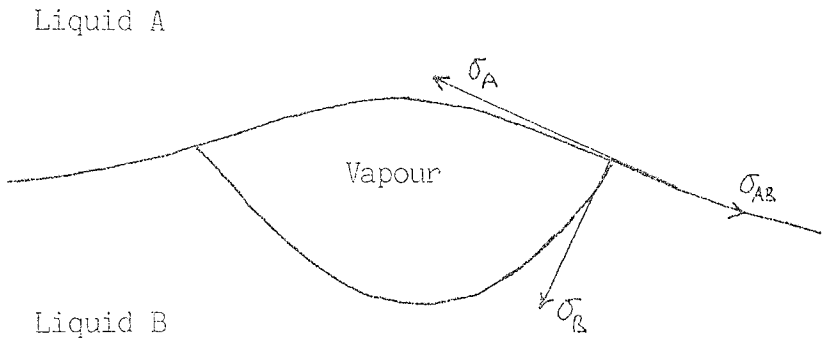

Fig. (2.02) The lenticular - shaped vapour embryo at a liquid-liquid interface.

The effective surface tension is given by Z

(2.08)

$$Z = \left[\tfrac{1}{2}(\sigma_A^3 + \sigma_B^3) + \frac{1}{16}\sigma_{AB}^3 + \tfrac{3}{8}\frac{\sigma^2_A\,\sigma^2_B}{\sigma_{AB}} - \tfrac{3}{8}\sigma_{AB}(\sigma_A^2 + \sigma_B^2) - \frac{3}{16}\frac{\sigma_A^4 + \sigma_B^4}{\sigma_{AB}} \right]^{1/3}$$

hence the expression for the superheat limit for a liquid-liquid system can be written as

$$T_L - T_{sat} = \frac{T_{sat}}{P_v L_v} \left(\frac{16 \pi Z^3}{3KT_L \ln\left(\frac{(Ck\, T_L)}{h}\right)} \right)^{\frac{1}{2}} \qquad (2.09)$$

Pool Boiling Crisis

Boiling crisis is a sudden drop of heat transfer coefficient occurring after a very high heat flux in nucleate boiling has been reached. The physical description of boiling crisis in pool boiling is that when the heat flux and liquid superheat increase the active nucleation sites become so numerous that the bubbles at the surface coalesce to form a blanketing layer of vapour.

Rohsenow and Griffith (48) obtained a correlation of the critical flux:

$$\frac{q'_{crit}}{L_v P_v} = 143 \left(\frac{\rho_l - \rho_v}{\rho_v} \right)^{0.6} g^{\frac{1}{4}} \quad \text{ft/hr} \qquad (2.10)$$

Zuber (49) postulated that boiling crisis is due to a Helmholtz instability. The correlation may be written as:

(2.11)

$$\frac{q'_{crit}}{L_v P_v} = \frac{\pi}{24}\left(\frac{\sigma(\rho_L - \rho_v)\, g g_c}{\rho_v^2}\right)^{\frac{1}{4}}\left(\frac{\rho_L}{\rho_L + \rho_v}\right)^{\frac{1}{2}}$$

Where g_c is a conversion ratio.

Addoms (50) has suggested a correlation for pool boiling crisis as:

(2.12)

$$q'_{crit} = 2.4\, L_v \rho_v \left(\frac{\rho_L - \rho_v}{\rho_v}\right)^{\frac{1}{2}}\left(\frac{K}{\rho C_p}\right)^{\frac{1}{2}}$$

Chang and Snyder (51) have used wave motion theory and suggested a correlation for predicting the pool boiling critical heat flux.

(2.13)

$$q'_{crit} = \frac{\pi}{12} L_v \rho_v^{\frac{1}{2}}\left(\frac{\rho_L + \rho_v}{\rho_L}\right)^{\frac{1}{2}}\left(g g_c \sigma(\rho_L - \rho_v)\right)^{\frac{1}{4}}$$

Kutateladze (52) has developed a critical heat flux correlation in saturated pool boiling by using dimensional analysis, and obtained the following correlation.

$$q'_{crit} = K^{\frac{1}{2}} \left[L_v (\rho_v)^{\frac{1}{2}} \left(\sigma g_c (\rho_L - \rho_v) g \right)^{\frac{1}{4}} \right] \qquad (2.14)$$

Where the average value of $(K)^{\frac{1}{2}}$ was found by experiment to be 0.14.

This correlation was extended to subcooled liquids by Zuber (53) who included a conduction term to account for the intermittent contact of subcooled fluid and heating surface. This results in the following ratio:

$$\frac{q'_{crit\ subcooled}}{q'_{crit\ saturated}} = 1 + \frac{5.3}{L_v \nu} \times \sqrt{k_c \rho_L C_p} \times \left[\frac{g(\rho_L - \rho_v)}{g_c \sigma} \right]^{\frac{1}{4}} \times \left[\frac{\sigma g g_c (\rho_L - \rho_v)}{\rho_v^2} \right]^{-\frac{1}{8}} (T_{sat} - T_{sub}) \qquad (2.15)$$

Kutateladze and Schneiderman (54) have found that equation (2.15) agrees with the critical flux in pool boiling of subcooled water and ethanol at less than 142 psia.

Film Boiling

Immediately after critical heat flux is reached, the boiling mechanism becomes unstable. This regime is called partial film boiling or transition boiling. Westerwater and Santangelo (55) have observed from high speed motion pictures

that vapour is formed in transition boiling by explosive bursts that occur at random locations and at high frequency. As the heater temperature increases further, boiling heat transfer again becomes stable, and stable film boiling occurs. The surface is so hot that the rapid evaporation of vapour forms a stable vapour interface which prevents the liquid from wetting the surface. The minimum surface temperature for this to occur is termed the Leidenfrost point (23). Bromley (56) presented a complete derivation for film boiling outside a horizontal tube in a pool. The equation is:

$$h_{crit} = 0.62 \left[\frac{k_v^3 \, (\rho_L - \rho_v) \, L_v g}{D \mu_v (Tw - Tsat)} \right]^{\frac{1}{4}} \qquad (2.16)$$

Where the coefficient of 0.62 is empirical, μ_v is the vapour viscosity.

The equation becomes invalid for both very small and very large values of D.

Berenson (57) has derived an analytical expression for the heat-transfer coefficient near the minimum heat flux in film pool boiling from a horizontal surface. The expression is:

$$h_{crit} = 0.425 \left[\frac{K_v^3 \, (\rho_L - \rho_v) \, L_v g}{\mu_v (T_w - T_{sat}) \sqrt{\frac{g\sigma}{g(\rho_L - \rho_v)}}} \right]^{1/4} \qquad (2.17)$$

The major difference between Berenson's and Bromleys results is the substitution of:

$$\sqrt{\frac{q_o \sigma}{g(\rho_L - \rho_V)}} \tag{2.18}$$

for the tube diameter D.

Equations 2.16 and 2.17 agree with experimental data for n-pentane and carbon tetrachloride, but not however for water.

Chapter III

Fuel Coolant Interaction Theories

Vaughan (58) has classified some sixteen interaction theories into six basic areas. These areas are:

a). Spontaneous nucleation of coolant.

b). Entrapment of coolant by fuel.

c). Boiling dynamics of coolants.

d). Hydrodynamics of the fuel and coolant.

e). Liquid to solid phase change of the fuel.

f). Incondensible gas release.

Some of the fuel coolant theories that have been proposed are briefly outlined in this chapter, and are summarized in table 3.01.

Spontaneous Nucleation Theories

As noted in Chapter II, a liquid when heated typically boils at a temperature T_{sat} at which its vapour pressure equals the ambient pressure. However it is possible to heat a liquid to a temperature in excess of T_{sat} without inducing a phase change in the bulk liquid. The maximum temperature to which a liquid can be heated at a given pressure is termed T_{hom} the super heat limit, and at this temperature thermodynamic fluctuations lead to bubble formation and bulk boiling. The temperature a given liquid is observed to boil at is termed T_{spon} that is the spontaneous nucleation temperature. In a system deficient in nucleation sites T_{spon} will lie close to T_{hom}, hence when boiling occurs it may be explosive because large amounts of thermal energy will be latent in the superheated coolant. The superheat theory was introduced and applied to the results of water/cryogen experiments by Nakanishi and Reid (59) and Katz and Sliepcevich (60). Fauske (20) developed the theory and generalised it to include other materials, forwarding the statement that large scale energetic explosions cannot occur if the instantaneous contact temperature is less than the spontaneous nucleation temperature of the coolant.

The basic superheat theory has been extended by Henry and Fauske (61) who have put forward the capture model; and Ochiai and Bankoff (62) have proposed the splash model. The capture model postulates that liquid coolant, in drop form and surrounded by coolant vapour is 'captured' on the fuel

surface resulting in high heat flux and rapid evaporation and condensation until explosive vaporisation occurs. The process is seen as cyclic and leads to a coherent explosion. The splash model assumes that when the interface temperature is above the spontaneousnucleation temperature random local contacts produce bubbles which coalesce into a high pressure vapour film which may collapse locally and transmit the impulse to the fuel. The resulting splash produces further liquid-liquid contact and propagation through the film occurs.

Coolant Entrapment Theories

Long (63) has proposed an entrappment theory to explain the results of experiments consisting of molten aluminium poured onto containers of water. In such experiments interaction appeared to occur as the metal settled to the bottom of the water container. If the molten metal enters the water and remains basically in a single body while settling to the bottom, water may be 'trapped' between the hot molten metal and the container surface. The thermal energy of the molten metal vaporises the trapped coolant, and the vaporised coolant expands fragmenting the molten metal. The fragmentation produces a greatly increased surface area thus enabling high heat fluxes to develop and so form an explosive interaction.

Hess and Brondyke (64) have extended the work of Long (63) by the use of high speed photography and greater aluminium superheats. Page (65) working with aluminium and copper has,

suggested that the molten metal need not stay as a bolus or coherent mass, but may be coarsely mixed with the coolant and depending on the heat transfer mechanism may then reform into a coherent mass on the container base. Interaction may be triggered by an external energy source, with the molten metal either falling through the water, coarsely mixed with the water, or as a coherent mass on the bottom of the container. Long (63), Hess and Brondyke (64) and Page (65) have all reported that coating the base of the container tended to prevent spontaneous explosions from the base of the container.

A jet formation model is supported by Buchanan and Dullforce (66) in experiments where a jet of coolant is fired into the molten metal or fuel, this results in an energetic interaction. It is thought that such a coolant jet can be formed by the asymmetric bubble collapse produced when a vapour bubble condenses into subcooled coolant. The resultant coolant jet is thought to penetrate the fuel surface, vaporise and throw out fuel particles into the coolant. The enhanced heat transfer rate causes a further bubble to grow and the sequence is repeated, with greater energy, in an escalating cycle until the fuel cannot supply the required heat because it has cooled, been dispersed or both.

Boiling Dynamics Theory

From a consideration of boiling dynamics there are two regions of boiling heat transfer that are intrinsically violent; these

are nucleate boiling, and transition film boiling. Swift (67) proposed that the violence associated with nucleate boiling causes fragmentation of the molten metal. In transition film boiling the heat flux increases as the fuel temperature cools, making it an inherently unstable situation. It has been suggested that these forces are sufficient to cause disruption of the fuel which would lead to an explosion. Board et al (68) and (69) studied tin/water interactions and noted that the vapour film which separated the molten tin from the water underwent oscillation. High speed film indicated that the vapour film collapsed completely onto the hot tin surface. It was proposed that as the vapour film collapses liquid coolant contacts the metal surface and is vaporised, fragmenting the molten metal. A refinement of this mechanism is Kazimi's hypothesis (70) that acoustic cavitation was the fragmentation mechanism for near-spherichal metal droplets cooling in water. Acoustic cavitation is a phenomenon whereby the molten metal experiences significant reductions in pressure in response to an oscillating vapour region adjacent to the fuel. If the pressure was reduced appropriately, cavitation of the molten metal could occur.

Experimental observations by Stevens and Witte (71) of the behaviour of moving, heated spheres in a coolant have shown that the mode of breakdown of stable film boiling to transition film boiling is dependent on the bulk coolant temperature. For low subcooling the breakdown was called 'progressive

instability', while for large subcoolings it was called 'precipitous collapse' as it occurred over a much shorter time scale.

Hydrodynamic Theories

Hydrodynamic forces can occur when two fluids in relative motion are in contact with each other. Witte, Cox and Bouvier (72) have suggested fragmentation by pure inertial forces. The governing relationship for this type of instability is the so called Weber number We, where:

$$We = \frac{\text{inertia forces}}{\text{surface tension forces}} = \frac{\rho_c DV^2}{\sigma} \qquad (3.01)$$

where ρ_c = density of coolant

D = fuel droplet diameter

V = fuel droplet velocity

σ = fuel surface tension

At high relative velocities Taylor instability has been suggested by Theofanous, Saito, and Efthimiadis (73) to cause fragmentation. Baines (74) notes that hydrodynamic fragmentation is more easily quantified than vapour collapse or vigorous boiling, and that it is of particular interest in sodium/UO_2 systems because it does not depend on detailed nucleation behaviour.

Hydrodynamic theory can be applied to the boiling process and Lamb (75) and Zuber (76) have applied Helmholtz instability to a vertical vapour jet, to show that the maximum vapour velocity for a stable vapour stream from a hot surface is given by:

(3.02)

$$V_v = \left[\frac{\rho_L \sigma m k}{\rho_v (\rho_L + \rho_v)} \right]^{\frac{1}{4}}$$

Where V_v is the vapour velocity

ρ_v is the liquid coolant density

ρ_v is the vapour density

σ is the surface tension

k is a conversion ratio 16ft/lb hr^2

m is the wave number given by:

$$m = \frac{2\pi}{\lambda}$$

If the vapour stream velocity exceeds this value, vapour cannot easily get away and thus a partial vapour blanketing may occur, that is the onset of transitional film boiling.

The criterion for stable film boiling on a horizontal surface facing upwards can be developed from the Taylor instability. The stability of an interface of wave form, that is a capillary wave, between two fluids of different densities depends upon the balance of the surface tension energy and the sum of the kinetic

and potential energy of the wave. Whenever the former is greater than the latter, a lighter fluid can remain underneath the heavier fluid, which is the condition of stable film boiling from a horizontal surface. This is illustrated in figure 3.01

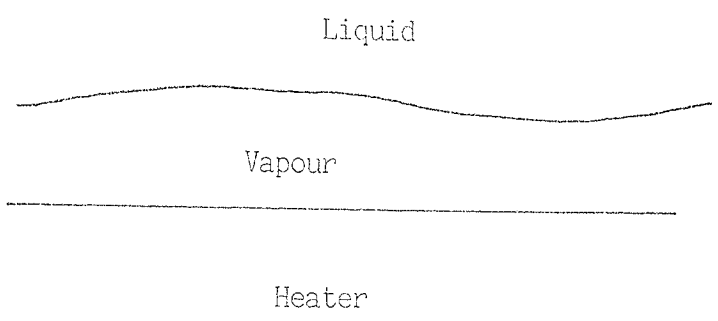

Figure 3.01. Stable Vapour Film.

According to Lamb (75) the total energy per wavelength of a progressive wave due to kinetic and potential energy is:

(3.03)

$$\left(\frac{E}{\lambda}\right)_{KE+PE} = \frac{g(\rho_L - \rho_V)\eta_o^{\,2}}{2K}$$

where g is the acceleration due to gravity

η_o is the maximum amplitude of the wave. The energy of the wave due to surface tension is:

(3.04)

$$\frac{E}{\lambda} = \frac{1}{\lambda}\int_0^{\lambda} \Delta P\, \eta\, dx$$

Where ΔP is the pressure differential for a curved surface. It can be shown that the condition of a stable wave is that

$$\left(\frac{E}{\lambda}\right)_{KE+PE} < \left(\frac{E}{\lambda}\right)_{\sigma}$$

Hence for stable film boiling,

$$\lambda < 2\pi\left(\frac{g_c\,\sigma}{g\,(\rho_L - \rho_V)}\right)^{\frac{1}{2}} \qquad (3.05)$$

In a physical system the disturbance wavelength λ can be interpreted as the distance between nucleation sites or as the departure bubble size.

The nomenclature for equations 3.03 to 3.05 follows that of equation 3.02.

Fuel Phase Change Theories

Fuel phase change theories appear to hinge on the solidifying outer shell of the initially molten metal droplet, cracking and releasing pressurised molten metal from the droplet core. Zyszkowski (77) and (78) experimenting with copper and highly subcooled water, postulated a 'jetting' mechanism of molten metal protruding through the vapour layer into the coolant and causing a localized region of rapid cooling. This rapid cooling

then produced a rapid crystalline structure change, with material fragmentation. However Knapp and Todreas (79) have reported that a metal could be plastic and not brittle at its melting point, and Flory, Paoli and Mester (80) have found that bismuth/water systems undergo F.C.I.'s in a similar manner to other metal/water systems but bismuth expands on freezing.

Incondensible Gas Release

This mechanism was first put forward by Epstein (81) and (82) and it is based on the assumption that dissolved gasses are present in the molten fuel. On rapid cooling the fuel becomes supersaturated with gas which pressurizes the hot liquid interior and results in dispersal of small particles of fuel into the coolant. The mechanism is applicable to the original experiment, that of atomic oxygen dissolved in silver. Baker and Ward (83) suggest that it would also be applicable for oxygen dissolved in steel. However, many F.C.I. experiments have been conducted under an inert gas atmosphere and Johnson and Shuttleworth (84) have pointed out that the amounts of inert gas that can be dissolved under such conditions would be very small.

Table 3.01

Summary of F.C.I. Theories (after Vaughan (58))

Theory	Basic Area
Superheat Capture model Splash model	Spontaneous nucleation theories.
Coolant entrapment Jet formation	Coolant entrapment
Violent boiling Collapsing vapour bubble Oscillating Vapour blanket Cavity formation	Boiling dynamics
Inertial forces Colgate mechanism BNL propagation model	Hydrodynamics
Shell theory Surface Cracking & Fissures Zyszkowski model	Fuel freezing, phase change
Incondensible gas release	Physical Chemistry

This review is not detailed or complete but it does provide an indication of the wide and varied fuel coolant interaction theories that have been proposed, and how this complex area can be approached from different conceptual viewpoints.

Chapter IV

Experimental Apparatus

Introduction

To enable experimental heat transfer rate data to be recorded for molten metal/water systems, suitable apparatus had to be designed and constructed. Previous workers in this field had used solid heaters with various geometries. For example Berenson (57) has used a horizontal plate, Bromley (56) used a vertical plate, Frederking and Clark (85) a solid sphere, Caldarola and Ladisch (86) a solid cylinder with a spherical lower end, Konuray (87) a solid sphere and crucibles of molten tin, Dullforce (88) molten drops of tin on a thermocouple junction, and Nelson and Buxton (89) of Sandia Laboratories melted various metals and oxides in a floodable arc-melting apparatus.

The above over-view does not claim to be complete or representative of heat transfer experiments, but merely as an outline of the various experimental approaches that have been made.

Apparatus was designed and built based on Nelson and Buxton's floodable arc-melting apparatus, but with a different mode of heating, and a different melt containment geometry and without a flash X-ray imaging facility. The apparatus that was built enabled molten metal to be flooded with pre-heated water. A crucible which contained the metal was held in a refractory base in such a way that the surface of the metal was flush

with the tank bottom. A glass sleeve, mounted on a stainless steel tube, was set round the crucible. When the sleeve was lifted, water from the tank flowed over the surface of the molten metal. A high speed thermocouple was passed through the base of the crucible so that temperature changes could be recorded.

Description of Apparatus

Temperature Measurement

An exposed junction thin wire chromel-alumel thermocouple encased in a glass fibre sheath was attached to a small crucible by passing the bare wires of the thermocouple through a short ceramic tube which pierced the base of the crucible. The ceramic tube was circular in cross section and contained two parallel internal bores. The tube was bonded to the crucible with refractory cement. The hot junction of the thermocouple was arranged to be a nominal 2.5×10^{-3}m below the surface of the metal contained in the crucible, while the cold junction was maintained at $0^{\circ}C$ in an ice bath. Copper extension leads connected the cold junction to a Datalab 905 transient recorder and to a potentiometer used for calibration purposes. A double pole, double throw switch connected the extension leads to a temperature gauge in such a way that either the gauge was connected to the leads, and the transient recorder and potentiometer were not connected, or that the gauge was not connected, but the transient recorder and potentiometer were. The potentiometer and transient recorder both had isolation

switches to enable independent use.

A thermocouple was used as a temperature sensor because it was decided after consideration that a thermocouple offered numerous advantages over other temperature transducers. Physically, a thermocouple is inherently simple, being only two wires joined together at the measuring end. It can be made large or small depending on the life expectancy, drift, and response-time requirements. A thermocouple normally covers a wide range of temperatures and its output is reasonably linear over portions of that range. Chromel-alumel thermocouples are fairly linear especially for a low cost base metal couple. Improved linearity can be found in platinum/ rhodium couples but these have a smaller Seebeck coefficient. Table 4.01 overleaf illustrates this.

Table 4.01 Nominal Seebeck Coefficients from reference (90)

Temperature	Thermocouple Type.				
	E	J	K	S	B
Deg.C	Seebeck Coefficient in Microvolts/Deg.C				
-190	27.3	24.2	17.1	-	-
-100	44.8	41.4	30.6	-	-
0	58.5	50.2	39.4	-	-
200	74.5	55.8	40.0	8.5	2.0
400	80.0	55.3	42.3	9.5	4.0
600	81.0	58.5	42.6	10.3	6.0
800	78.5	64.3	41.0	11.0	7.7
1000	-	-	39.0	11.5	9.2
1200	-	-	36.5	12.0	10.3
1400	-	-	-	12.0	11.3
1600	-	-	-	11.8	11.6

The thermocouple element construction material for the five thermocouple types listed in table 4.01 can be found below in table 4.02.

Table 4.02 Common Thermocouple Types from reference (90)

Type	Material
E	Chromel (+) Constantan (-)
J	Iron (+) Constantan (-)
K	Chromel (+) Alumel (-)
S	Platinum/10% Rhodium (+) Platinum (-)
B	Platinum/30% Rhodium (+) Platinum/6% Rhodium (-)

In addition, unlike many temperature transducers thermocouples are not subject to self-heating problems and in practice thermocouples of the same type are interchangeable within specified limits of error.

Melt Containment

As the hot liquid used was a molten metal and the coolant water, a substantial temperature gradient over a short time interval was envisaged, and containment material which could tolerate thermal stress, molten metal attack, and was impervious to water was sought. Initial experiments involving tin at low

superheats were conducted using small nickel crucibles measuring 2.0×10^{-2}m in diameter by 2.5×10^{-2}m in height. For high metal temperatures nickel was found to be unsatisfactory due to liquid metal attack, and quartz crucibles of the same size were used.

Miller (91) notes that liquid-metal corrosion may take place by several fairly common mechanisms, which include a relatively uniform solution attack on the solid surface, and an attack by direct alloying. Attack in a specific area can be due to intergranular penetration which results from a selective reaction of the liquid metal with minor constituents of the solid. This can drastically alter the physical properties of a material without appreciably changing its appearance. Also, thermal-gradient transfer can occur by the coexistence of a temperature differential and an appreciable thermal coefficient of solubility. Even though the actual solubility may be quite low, appreciable amounts of a solid component may be dissolved from the zone of higher solubility and precipitated in the zone of lower solubility.

Miller (91) in a review of containment materials for molten aluminium concludes that almost all solid metals and alloys are severely attacked and are unsuitable for long-term contact with molten aluminium. Molten lead especially at 1000°C and above is also difficult to effectively contain in a solid metal closure though at lower temperatures many metals and

alloys have good resistance to attack. Liquid lead appears to promote mass-transfer attack at elevated temperatures. Molten tin attack is by intergranular penetration and direct solution, and is similar to molten aluminium, though less severe. Molten aluminium, lead, and tin were not reported to attack quartz. An oxygen-natural gas torch was used to heat the crucible.

Coolant Containment

A rectangular tank of base dimensions 2.0×10^{-1}m square and 1.4×10^{-1}m high was made. The base of the tank was cut from Asbestos 2.5×10^{-2}m in thickness. The centre of the base was recessed to a depth of 6.0×10^{-3}m and to a radius of 3.5×10^{-2}m. The centre was pierced by a hole of radius 3.0×10^{-2}m. The top surface of the Asbestos was sealed with a P.T.F.E. spray to water proof it.

Perspex of thickness 3.0×10^{-3}m was cut to size and bonded to the base and to itself with a silicon rubber adhesive. The top edge of the tank carried an anti-splash lip of perspex of width 1.0×10^{-2}m. This also served as bracing to give the top of the tank added rigidity. Perspex was chosen for the sides of the tank so that visual observation could be made, and also that in the event of an experiment being terminated by a vigorous spontaneous interaction, the hazard of debris would be minimised.

A pyrophillite collar 5.0×10^{-3} m thick and 3.4×10^{-2} m in radius was cemented into the recess in the Asbestos base.

The centre of the pyrophillite collar was recessed to a depth of 2.5×10^{-3}m and to a radius of 1.5×10^{-2}m. The centre was pierced by a hole of radius 1.3×10^{-2}m. A ring of pyrophillite 2.3×10^{-3}m thick and of radius to fit the recess of the collar was cemented to the collar. The centre of the ring was pierced by a hole of 1.0×10^{-2}m radius. This ring then received the crucible. The pyrophillite was machined in the 'green' state and then fired according to the manufacturers instructions.

The pyrophillite collar and ring were designed to provide a sub-assembly which would enable different sized crucibles to be fitted to the same pyrophillite collar by the use of different sized rings.

An electrical stirrer, with a speed control, was mounted in the tank as was an electrical immersion heater. The heater was controlled by a rheostat.

The Flooding Facility

The glass sleeve was made from a section of thin walled Pyrex tube, 1.2×10^{-1}m long and 8.0×10^{-2}m O.D. The tube was pierced by three equally spaced holes on its circumference in its lower section. Brass bolts were brazed onto lengths of brass studding and were used to attach the glass sleeve to the stainless steel carrier. The top and bottom edges of the sleeve were protected with a 'U' section rubber gasket. Where the glass was pierced for the brass bolts, the joints were made water tight by rubber 'O' rings,

one on each side of the glass, these also cushioned the glass from the brass bolts. To stop water seeping along the threads of the bolts, each unit was closed by brazing a small hexagonal brass plate to its outer face. The lower 'U' section gasket formed a water-tight seal against the pyrophillite collar when smeared with a little grease and under compression from a partially compressed coil spring. The 'U' section rubber gaskets were made from commercially available 'U' section rubber strip cut to length and bonded to form rings with cyanoacrylate adhesive and then water proofed with a proprietory agent.

The stainless steel carrier consisted of a disc which formed the top of the glass sleeve and the bottom stop of the compression spring, a tube of 2.0×10^{-2}m O.D. passed through the disc and was brazed to it. The tube acted as a former for the spring and passed through a brass bearing. The tube exhausted the glass sleeve to the atmosphere and carried a nylon delivery tube, 5.0×10^{-3}m O.D., of nitrogen. The brass bearing ensured that the assembly lifted in a vertical direction by limiting horizontal movement, and also acted as the top stop for the spring. The end of the tube carried a 'D' shackle attached via a pulley system to a heavy lead weight. The weight was held in an electrically operated bomb release unit, which when fired released the weight and thus lifted the glass sleeve. The mass of the lead weight was determined by experiment so that the compression spring

was not completely compressed thus cushioning the lift of the sleeve. The entire assemply was held in a framework of angle iron. Figure 4.01, below, is a cross-sectional diagram of the interaction vessel.

FIGURE 4.01 Cross section of Interaction Vessel (approx.half life size.

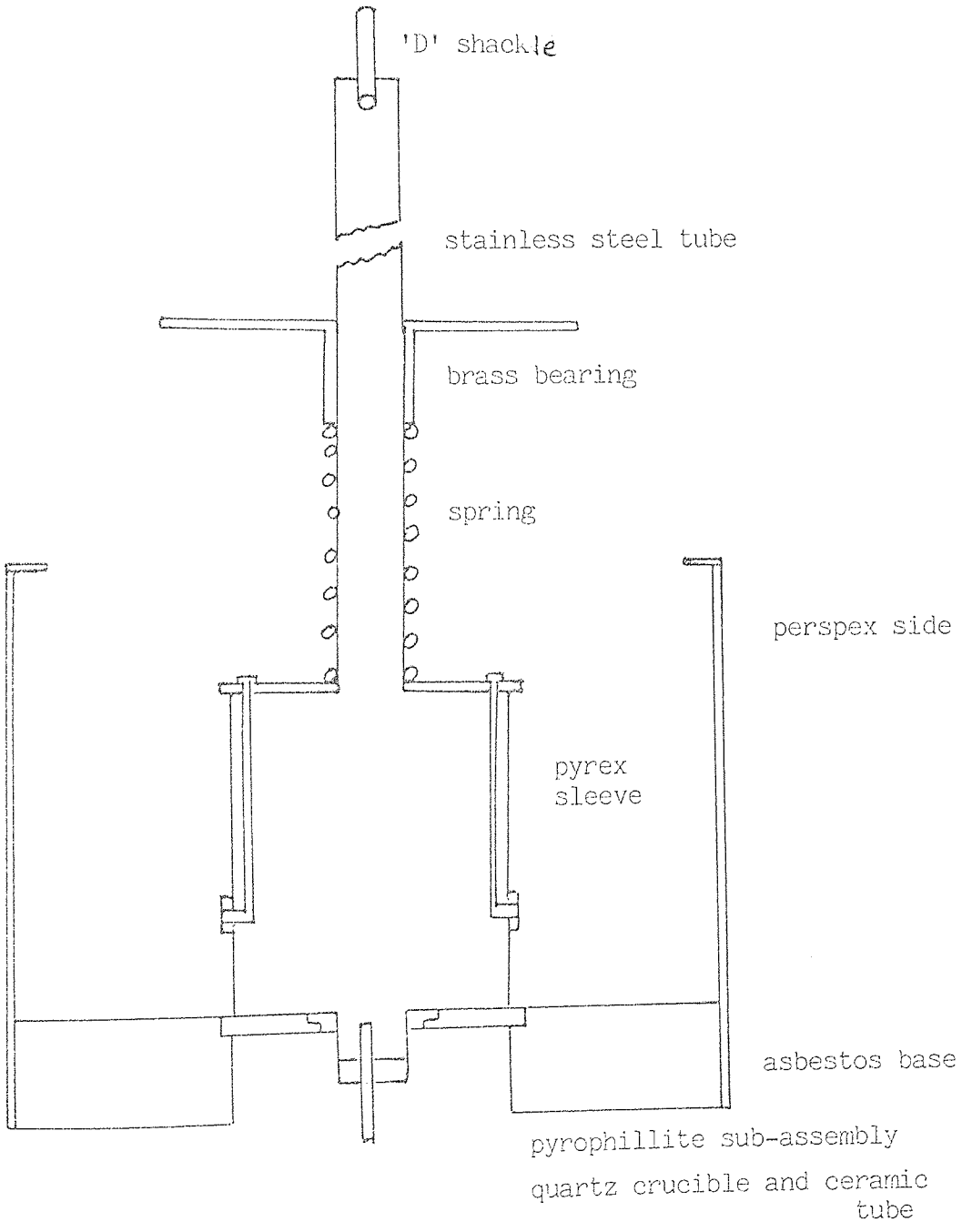

Data Recording

The thermocouple was connected to a double pole, double throw (D.P.D.T.) switch. The Seebeck e.m.f. from the couple could either drive a specially calibrated analogue temperature gauge, or a calibration potentiometer and transient recorder. The latter two instruments could be used independently of each other by the use of switches within the respective instruments.

The Datalab DL 905 transient recorder was used to store the experimental signal. The DL 905 consisted of a 5 M H_z, 8-bit analogue-to-digital converter (A.D.C.) connected to an 8-bit by 1024 word MOS shift register memory. The variable gain, wide band amplifier preceded the A.D.C. and a digital-to-analogue converter was used to reconstruct stored data back into analogue form. Data storage was permanent until a new record command was made or until power was removed from the instrument. The stored input signal from the thermocouple was displayed as a sustained trace on a cathrode ray oscilloscope monitor and was also outputted to a Rikodenki-Mitsui pen recorder so that a permanent record of the signal was obtained.

Figure 4.02, page 47, is a schematic wiring diagram of the apparatus.

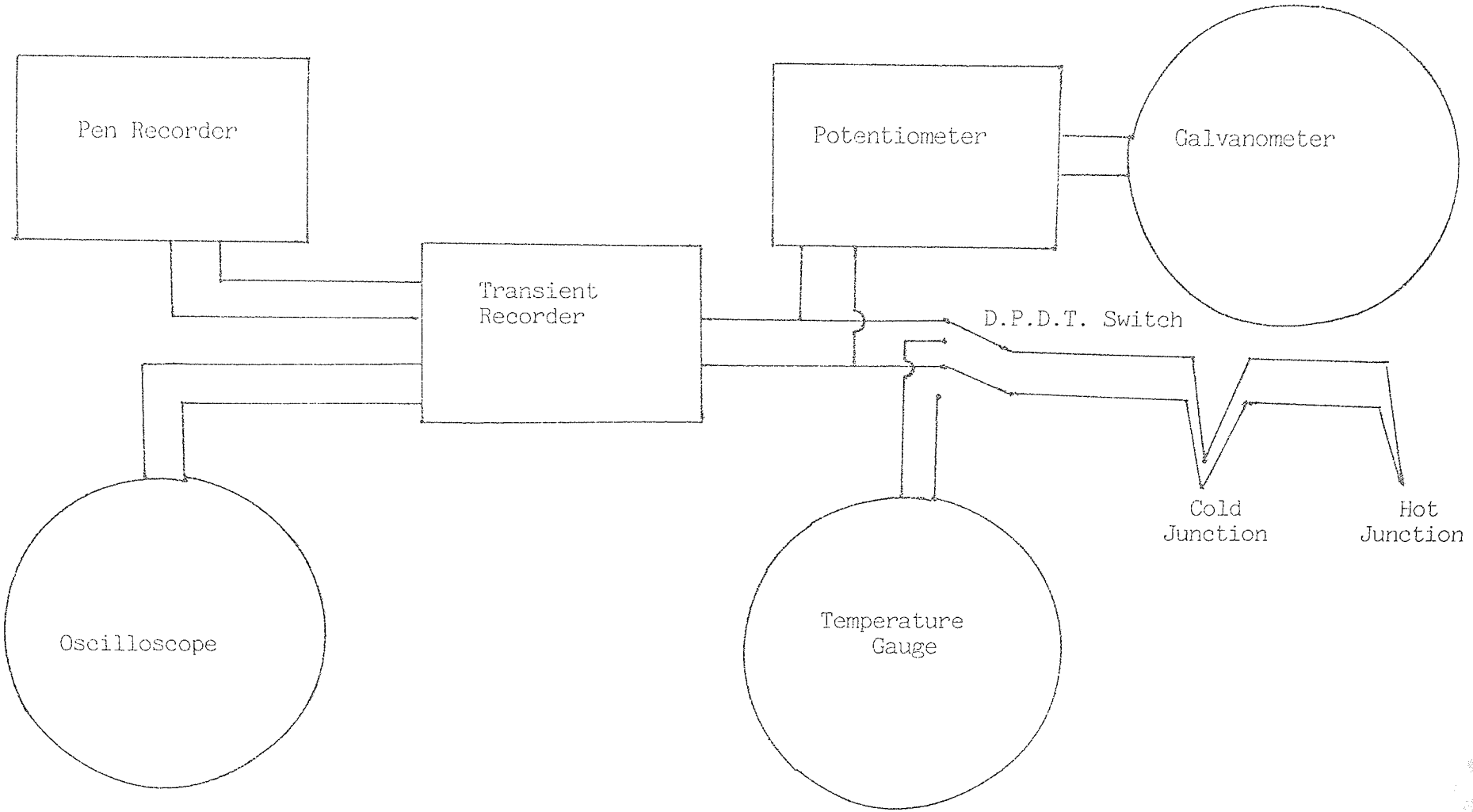

Figure 4.02 Schematic Diagram of Apparatus

Chapter V

Method of Experimentation

Setting Up

The glass sleeve and stainless steel carrier were removed from the interaction vessel. The tank was cleaned and dried. The pyrophallite collar and ring were cemented to the base of the tank and gently heated with the oxygen-natural gas torch to drive off the water. When the cement was dry it was strongly heated to effect a cure. It was then left to cool.

A quartz crucible was carefully fitted into the pyrophillite sub-assembly and the ceramic tube, which carried the thermocouple, was cemented into place so that the hot junction of the thermocouple was a nominal 2.5×10^{-3}m below the rim of the crucible. The ceramic tube and thermocouple were set in the central vertical axis of the crucible. The cement was heat curred as outlined above.

Metal granules, from a pre-weighed excess amount, were melted into the crucible under a nitrogen atmosphere. When the metal and the surrounding sub-assembly had cooled, a little grease was smeared on the lower rubber gasket on the sleeve, and the sleeve was then positioned over the crucible.

The DL 905 transient recorder was connected to an oscilloscope and a pen recorder, according to the

manufacturers instructions. An internal adjustment to the transient recorder/pen recorder interface board was made so that the data was outputted at a slower rate in order that the pen recorder could respond to the signal without being in dead time, that is the input signal speed was matched to the response characteristics of the pen recorder. Early experiments with the DL 905 indicated that when the recorder triggered and stored a signal the corresponding output signal was not a facsimile of the original signal, but contained an artifact from the triggering circuit. This stray signal was removed by the partial re-wiring of an internal circuit board following private communications (92) with the manufacturers.

Typically the DL 905 recorder was set so that its pre-trigger sweep rate was 2.0 ms and its post-triggered sweep rate was 10.0s. A delay setting of 50 was used so that the fraction 949/999 of the recorder's memory would be used for post-trigger signal storage. The volts full scale (v.f.s.) setting used for low melting metals and for low superheats was 0.02, while for higher melts and superheats the 0.05 setting was used. These two settings were found to maximise the sensitivity of the DL 905 and the pen-recorder.

The tank was filled to the required depth with water and brought to uniform temperature with the imersion heater and

stirrer. The water temperature was measured with a mercury thermometer. The crucible and the contained metal were heated with the torch under an atmosphere of nitrogen. For high temperature experiments two torches were used set opposite to each other. The approximate metal temperature was read from the analogue gauge, and an accurate calibration reading was made with the potentiometer. The e.m.f. corresponding to this temperature was recorded in the DL 905. The stored signal was then outputted to the pen-recorder, thus converting the given e.m.f. to vertical pen travel. The pen travel was then read and compared with a previously constructed calibration graph. Typically this reading fell within the standard deviation of the calibration graph and the experiment would proceed. If however the reading did not comply, then the experiment would be aborted and the thermocouple replaced.

When the required superheat was reached and the required coolant subcooling maintained, the heater and stirrer were switched off. The thermocouple e.m.f. output was transferred to the DL 905, that is both the potentiometer and analogue gauge were isolated. The DL 905 was then armed so that its memory was filled by the signal from the thermocouple. The bomb release mechanism was then activated so that the molten metal was flooded with coolant. A transient electrical signal from the release mechanism was used to trigger the recorder so that the changing e.m.f. of the thermocouple

replaced 949/999th of the memory of the recorder. The remaining 50/999th part of the memory still contained the effectively constant, pre-flooding, e.m.f. output of the thermocouple. It was found that the above procedure prevented the DL 905 from being triggered by random electrical transients from the other electrical equipment used in the experiment.

When the recording was made the DL 905 switched to a display mode and the experimental signal was observed on the C.R.O. monitor. The signal was then outputted, via an internal smoothing circuit in the DL 905, into the pen recorder. The horizontal travel of the pen recorder had been adjusted so that 2.0×10^{-1} m of travel was equivalent to 10 seconds. This gave a resolution of 5ms per 1.0×10^{-3}m.

The above experimental procedure was repeated with different metals and melt superheats, and with the coolant at different depths and temperatures. The metals used were tin, lead, and aluminium, and the coolant used was water.

Experiments were conducted with initial metal temperatures between approximately 600^{o}C and 1000^{o}C and with subcooled water at 95^{o}C to 5^{o}C. The lead/water experiments and the aluminium/water experiments were conducted with an initial depth of coolant of 5.0×10^{-2}m. The tin/water experiments were conducted with the initial depth of coolant varied between 10.0m x 10^{-2}m and 1.0×10^{-2}m.

Chapter VI

Experimental Results and Data Handling

Data from early trial experiments were initially processed in part with an electronic differentiator, and utilized the high gain two channel facility of the Rikadenti-Mitsui pen recorder. The differentiator was designed on a basic theoretical circuit from a R.S. Components data sheet. The theoretical circuit is set out in figure 6.01 below.

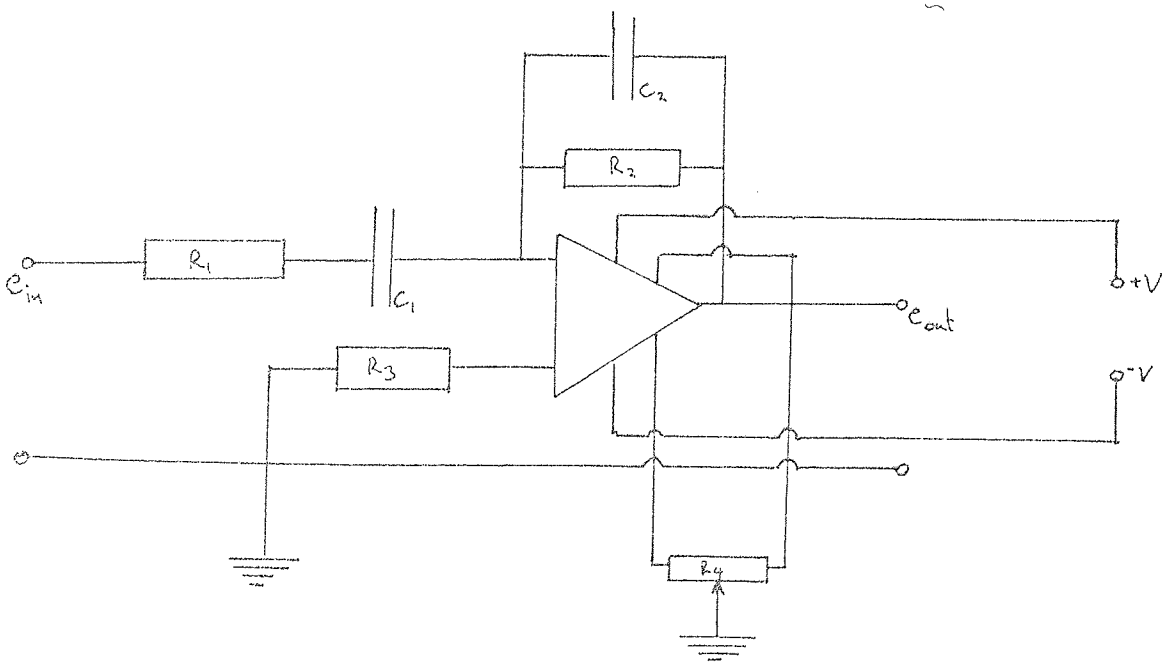

Figure 6.01 Schematic Theoretical Circuit.

The design characteristics of the device were such that upto a maximum input frequency f_{max}, which was determined by the

operational amplifier, a low frequency differentiator could be built, given the condition:

$$C_1 R_1 = C_2 R_2 \qquad 6.01$$

so that the time constants were equal.

Under conditions of equation 6.01 and at a frequency f_x, below f_{max}, the gain of the device would be given by:

$$\text{Gain} = \frac{R_2}{R_1} \qquad 6.02$$

and for a frequency f_x

$$e_o = C_1 R_1 \frac{d(e_1)}{dt} \qquad 6.03$$

where e_1 is the input voltage

e_o is the output voltage

At f_{max}

$$e_o = e_i \cdot \frac{R_2}{R_1} \qquad 6.04$$

Where f_{max}, the maximum frequency of operation is given by:

$$f_{max} = \frac{1}{2 \pi C_1 R_1} \qquad 6.05$$

From these relationships a practical circuit was designed based on the output rate of the transient recorder. The practical circuit with component values is set in figure 6.02

below:

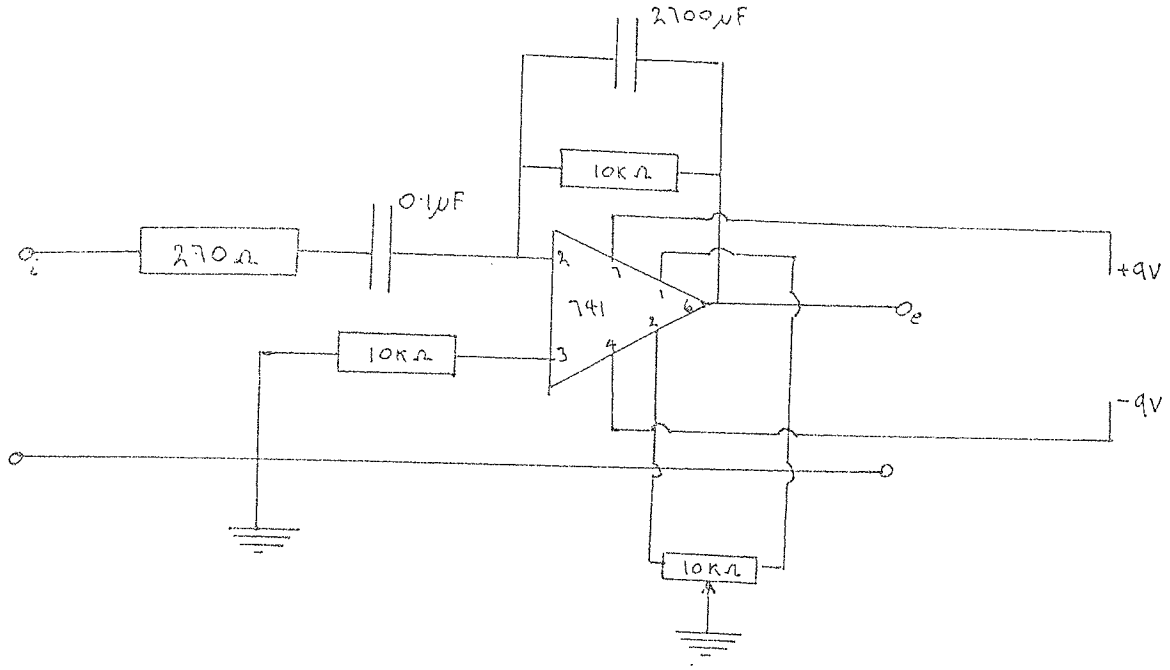

Figure 6.02 Schematic Practical Circuit.

An A.C. amplifier based on a practical circuit from a R.S. Components data sheet was constructed to amplify the output from the electronic differentiator. The device was tested with various wareforms from a signal generator. The differentiated trace and the original trace were compared on a double beam C.R.O. The device was found to perform satisfactorily for a wide range of signals and frequencies. A changing e m f output from a thermocouple set in a crucible of molten tin which was flooded with subcooled water, was stored in the DL 905. This signal was then outputted into the double channel pen recorder, one channel of which was via

the differentiator, so that a trace of the signal and its differential could be composed. However a technical difficulty was encountered in that the slow signal output rate of the transient recorder was too slow to drive the differentiator. The fast output rate of the continuous display mode to the C.R.O. monitor was found to drive the device, but the signal was outputted at too fast a rate for the pen recorder to follow. The device thus required a second DL 905 transient recorder to store the differentiated signal. However this facility was not available at the time of the experimentation. It was therefore decided to differentiate the experimental signal numerically.

Experiments yielded a plot of voltage against time. A calibration graph was constructed for both the voltage settings used, and calibration factors to convert volts to temperature (^{o}C) were obtained from these graphs. Time and temperature co-ordinates were drawn on each experimental trace obtained from the pen recorder. The time co-ordinates were divided into 500ms increments, which yielded a maximum of twenty-one data points. The bulk temperature of the molten metal was calculated from the vertical displacement of the experimental trace for each data point obtained. A linear regressions routine was used to assess the linear correlation between temperature and time. A correlation coefficient was calculated for each regression, and together with the sample size, was used to estimate the validity of the linear correlation. A validating

r_{test} routine yielded a percentage certainty for each correlation. The higher the percentage certainty, the more definite the correlation. Typically correlation coefficients of 99% and better were obtained. For coefficients of 95% and better, the average gradients and intercepts were calculated, as was the corresponding average temperature of the molten metal. From a knowledge of the cooling rate, geometry, mass and thermal properties a heat flux expression was derived, and heat fluxes were calculated for each experiment. An expression which yielded the metal surface temperature was also derived. A graphical correlation of heat flux,metal surface temperature and coolant temperature was obtained, as was a simplified linear correlation for the heat transfer coefficient and coolant depth.

The internal thermal energy of a body is defined by:

$$E = C\rho V T \qquad 6.05$$

Where E is the energy

C is the heat capacity

ρ is the density

V is the volume

T is the temperature

Assuming constant thermal properties and an isothermal body at any given instant in time, then a change in thermal energy ΔE will be given by:

$$\Delta E = C \rho V \frac{\Delta T}{\Delta t} \qquad 6.06$$

or $$\Delta E = C M \frac{\Delta T}{\Delta t} \qquad 6.07$$

where $\frac{\Delta T}{\Delta t}$ is the change in temperature with respect to time.

Hence, in a one dimensional conductive heat flow model the heat transfer rate q will be given by:

$$q = KA \frac{T_H - T_c}{x} = c m \frac{\Delta T}{\Delta t} \qquad 6.08$$

Now the heat flux q' is given by:

$$q' = \frac{q}{A}$$

Hence:

$$q' = k \frac{T_H - T_c}{x} = \frac{c m}{A} \cdot \frac{\Delta T}{\Delta t} \qquad 6.09$$

Where K is the thermal conductivity

A is the surface area of thermal contact

T_H is the hot temperature region)
T_c is the cold temperature region) of the molten metal

x is the distance between the two regions.

The physical system can be represented by figure 6.02 below:

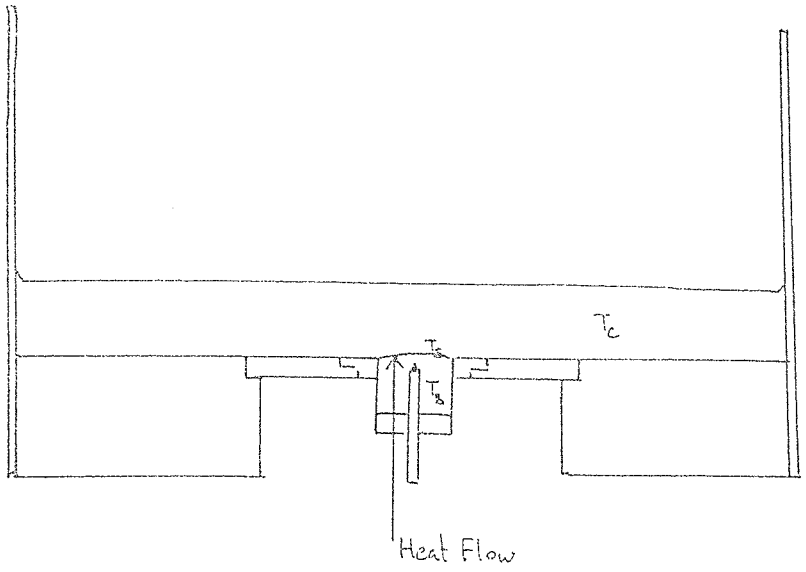

Heat can be envisaged as flowing out of the hot molten metal and into the coolant. In the case of a constant heat flux, a thermal gradient will occur in the metal and the thermocouple will not measure the surface temperature but will indicate the bulk temperature of the melt at some position x within the crucible.

Now the heat flow within the crucible is essentially along the vertical axis, and not radial. Therefore from equation 6.09 an expression for the surface temperature can be deduced, that is:

$$T_S = T_B - \left[\frac{CM}{Axk} \cdot \frac{\Delta T}{\Delta t} \right] \quad {}^{o}C. \qquad 6.10$$

Where T_s is the molten metal surface temperature

T_B is the molten metal bulk temperature

x is the distance between the metal surface and thermocouple hot junction.

C is the specific heat

M is the mass of metal

k is the thermal conductivity

$\frac{\Delta T}{\Delta t}$ is the rate of cooling

Now from a consideration of the simple energy balance:

Heat lost = Heat gained

It is clear that the rate of cooling of the metal will depend on the rate of heating of the coolant that is:

$$q = kA \frac{\Delta T}{\Delta x} = hA (T - T_\infty)$$

$$\text{or} \quad q' = k \frac{\Delta T}{\Delta x} = h (T_w - T_\infty) \qquad 6.11$$

Where h is the heat transfer coefficient

T_w is the hot surface temperature

T_∞ is the bulk coolant temperature T_c

Now q' can be calculated from equation 6.09, and T_w is T_s which can be calculated from equation 6.10. Hence a plot of q' against $(T_x - T_c)$ will yield h the heat transfer coefficient.

However, it is more usual to plot $\log_{10} q'$ against $\log_{10} \theta$ where $\theta = T_s - T_c$, and so produce the classical boiling curve of Farber and Scorah (25) which can be found in figure 2.01 page 8. The plot of $\log_{10} q'$ against $\log_{10} \theta$, is however different from that of many workers in the field of boiling heat transfer in that the heater or hot body was typically molten and that in all cases the initial bulk temperature of the water was always below boiling point. Subcooled water in the temperature range $5^{\circ}C$ to $95^{\circ}C$ was used for the molten lead and aluminium experiments while the earlier molten tin experiments were conducted with water in the temperature range $75^{\circ}C$ to $95^{\circ}C$ was used. Figure 6.03 is a compilation of $\log_{10} q'$ against $\log_{10} \theta$ for the three metals, aluminium, lead and tin, a curve of the relationship is drawn through the points and this curve is also drawn in part in figure 6.04 which are the results of the aluminium/water heat transfer experiments, and in full in figures 6.05 and 6.06 which are the results for the lead/ water and tin/water heat transfer experiments respectively.

The effect of coolant depth on heat transfer coefficients at coolant temperatures of 80°, 85°, 90° and 95° C were investigated with initial coolant depths of 1.0×10^{-2} m to 10.0×10^{-2}m. Final coolant depth was less than the initial depth due to the displacement of the glass sleeve. Table 6.01 is a table of initial and final depths.

Table 6.01										
Initial Depth (cm)	1.0	2.0	3.0	4.0	5.0	6.0	7.0	8.0	9.0	10.0
Final Depth (cm)	0.9	1.7	2.6	3.5	4.4	5.2	6.1	7.0	7.9	8.7

The relationship between the heat transfer coefficient and coolant depth is shown in figures 6.07 to 6.10.

Figure 6.03 Compilation of $\log_{10}$ Heat Flux against $\log_{10}\theta$ for

Molten Lead △ Subscript s denotes a solid/liquid

Molten Tin ○ interface

Molten Aluminium □

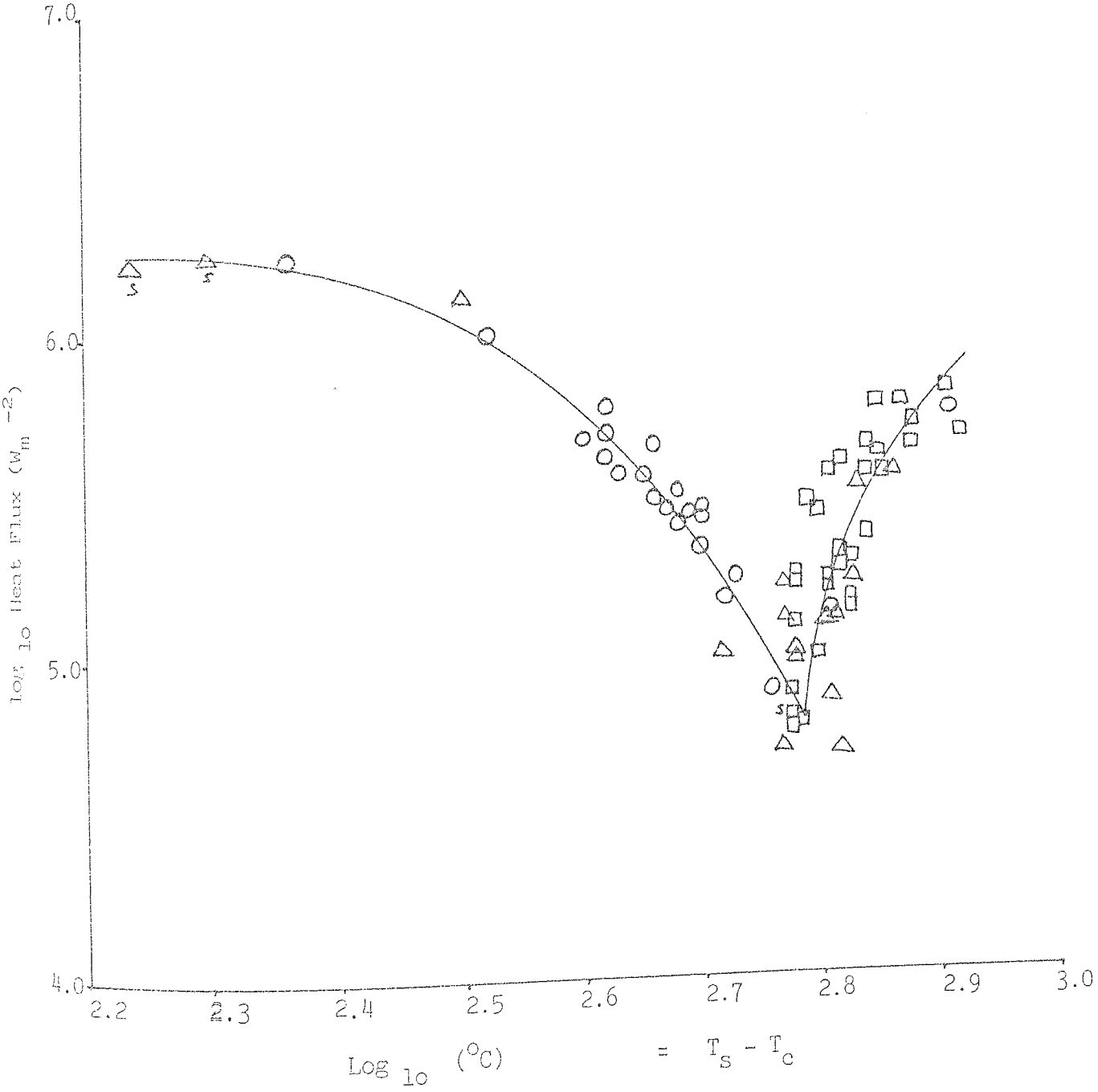

T_s is the surface temperature of the metal

T_c is the initial bulk temperature of the coolant.

Figure 6.04 Plot of $\log_{10}$ Heat Flux against $\log_{10}\theta$

Molten Aluminium/Subcooled Water

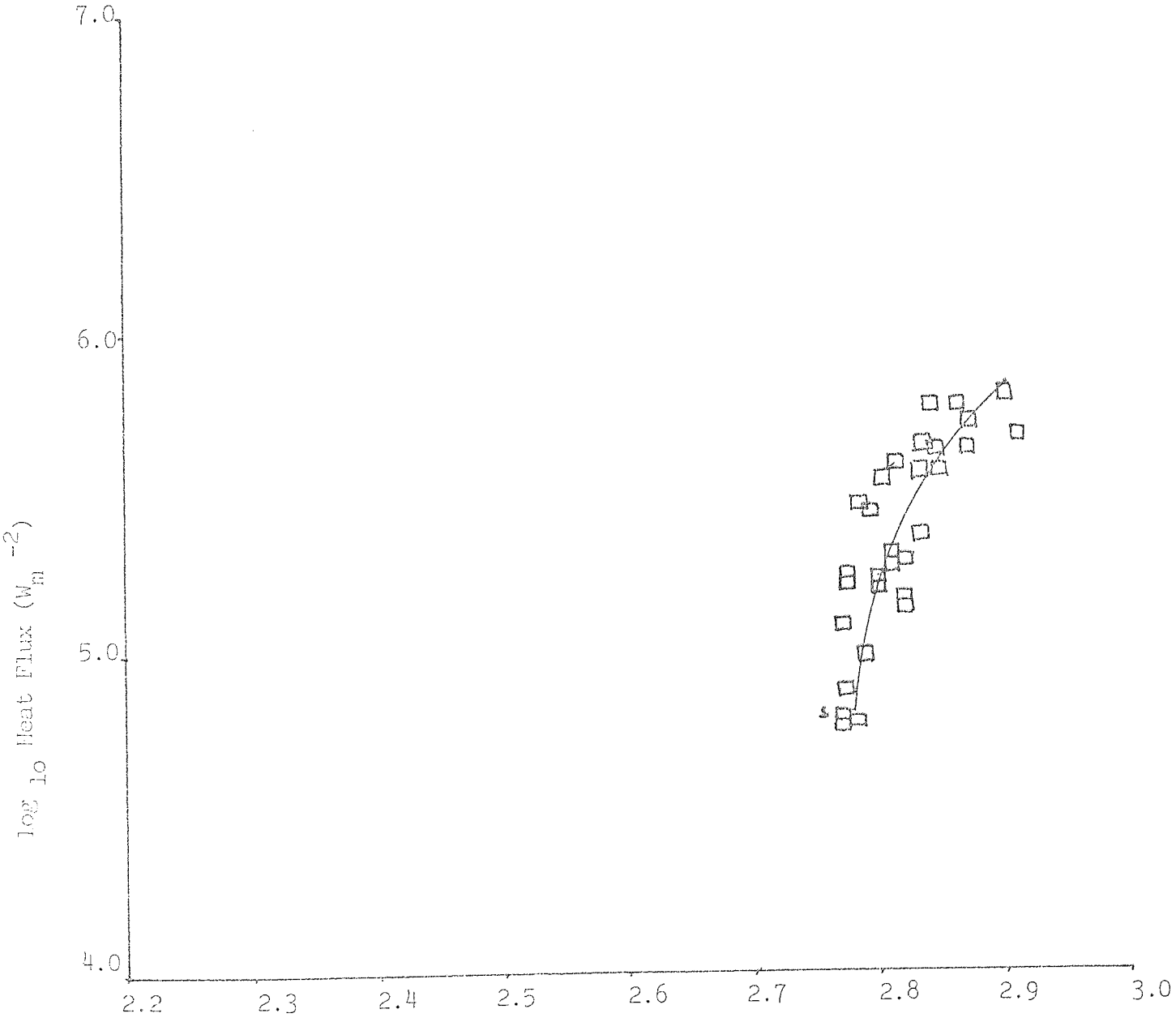

T_s is the surface temperature of the metal

T_c is the initial bulk temperature of the coolant.

Figure 6.05 Plot of $\log_{10}$ Heat Flux against $\log_{10}\theta$

Molten Lead/ Subcooled Water

Subscript s denotes a solid/ liquid interface

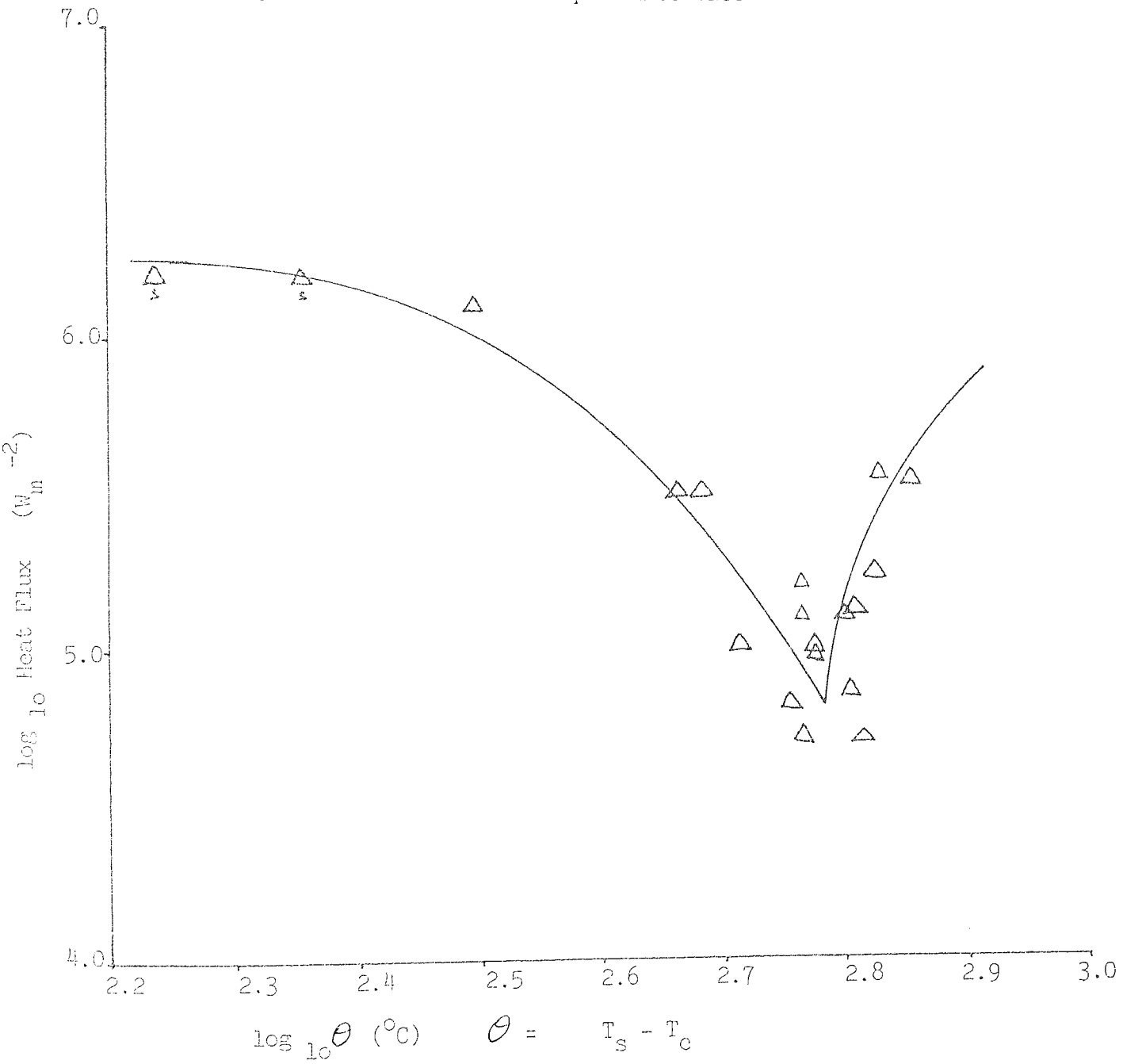

$\theta = T_s - T_c$

T_s is the surface temperature of the metal

T_c is the initial bulk temperature of the coolant.

Figue 6.06 Plot of $\log_{10}$ Heat Flux against $\log_{10}\theta$

Molten Tin/Subcooled Water

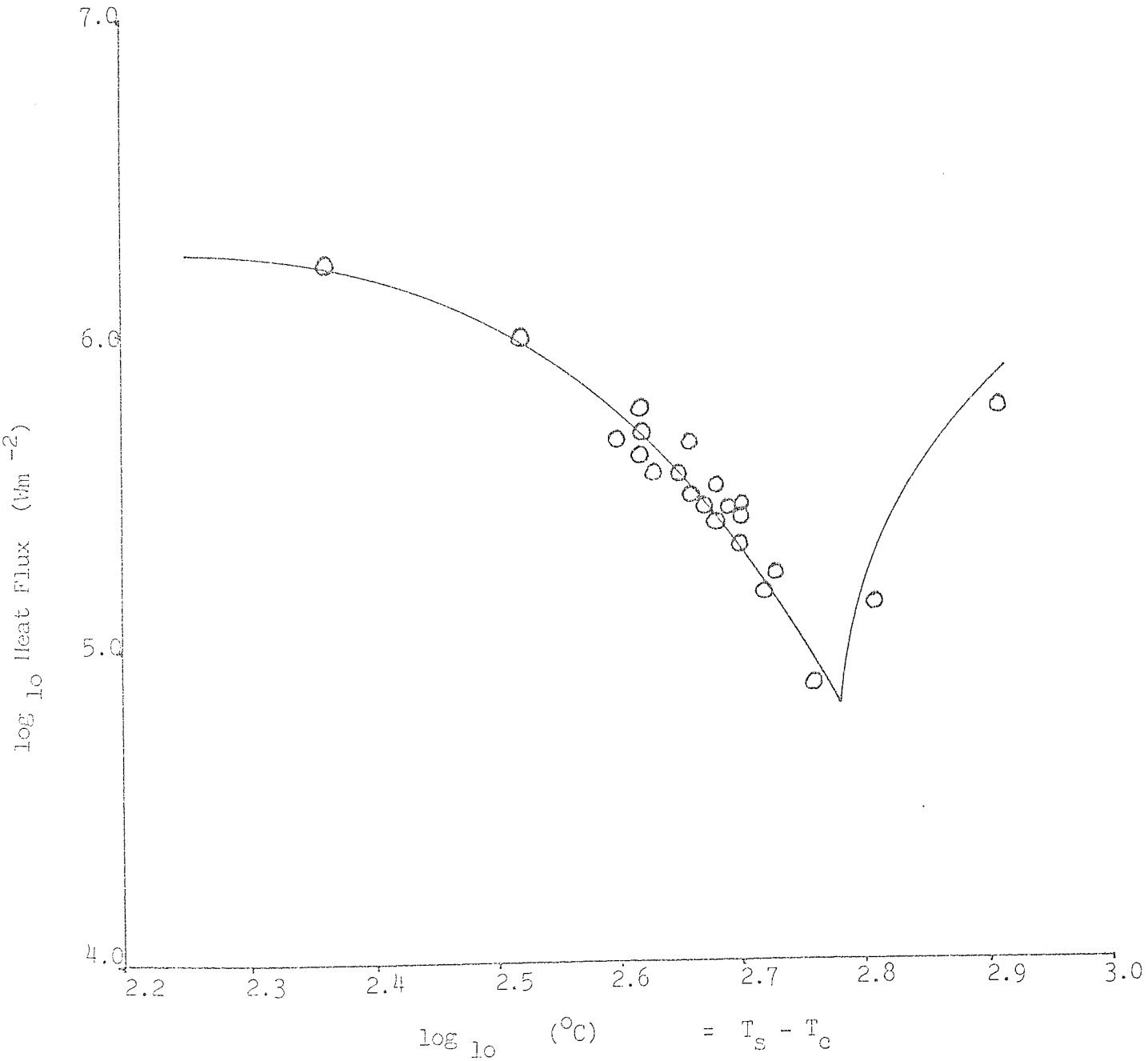

T_s is the surface temperature of the metal

T_c is the initial bulk temperature of the coolant

Figure 6.07 Plot of $\log_{10}$ Heat Transfer Coefficient (h) against Coolant Depth

Coolant Temperature 80°C

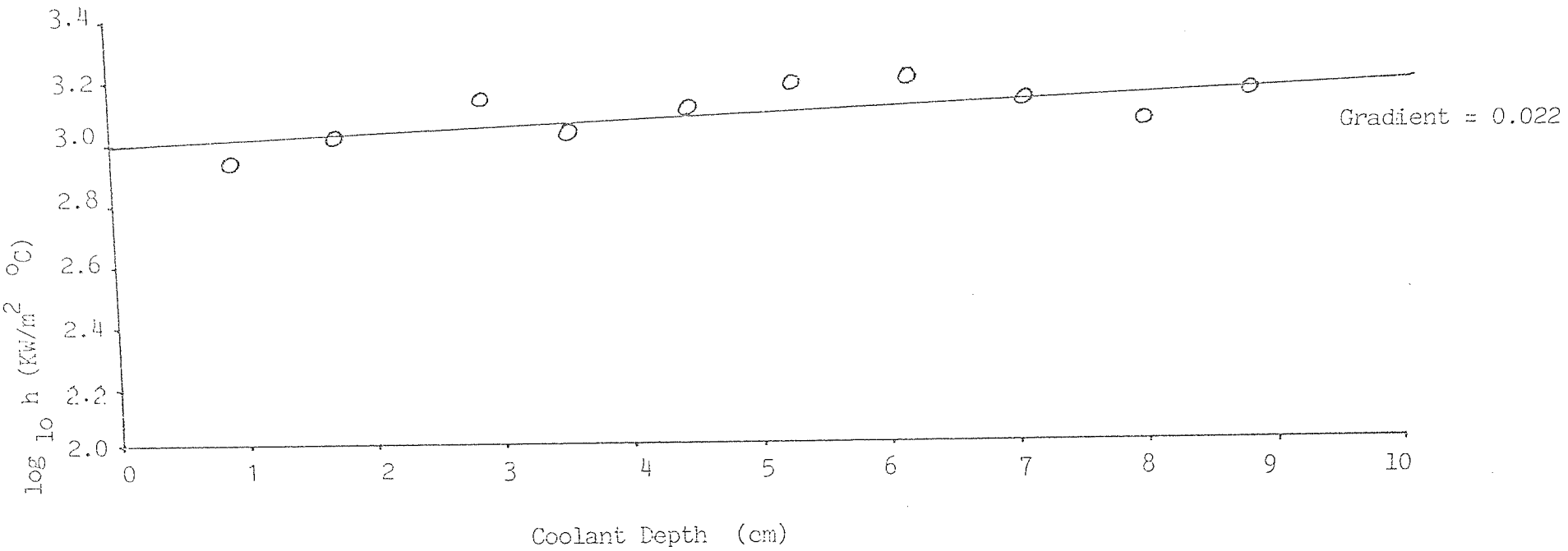

Figure 6.08 Plot of $\log_{10}$ Heat Transfer Coefficient (h) against Coolant Depth

Coolant Temperature $85^{o}C$

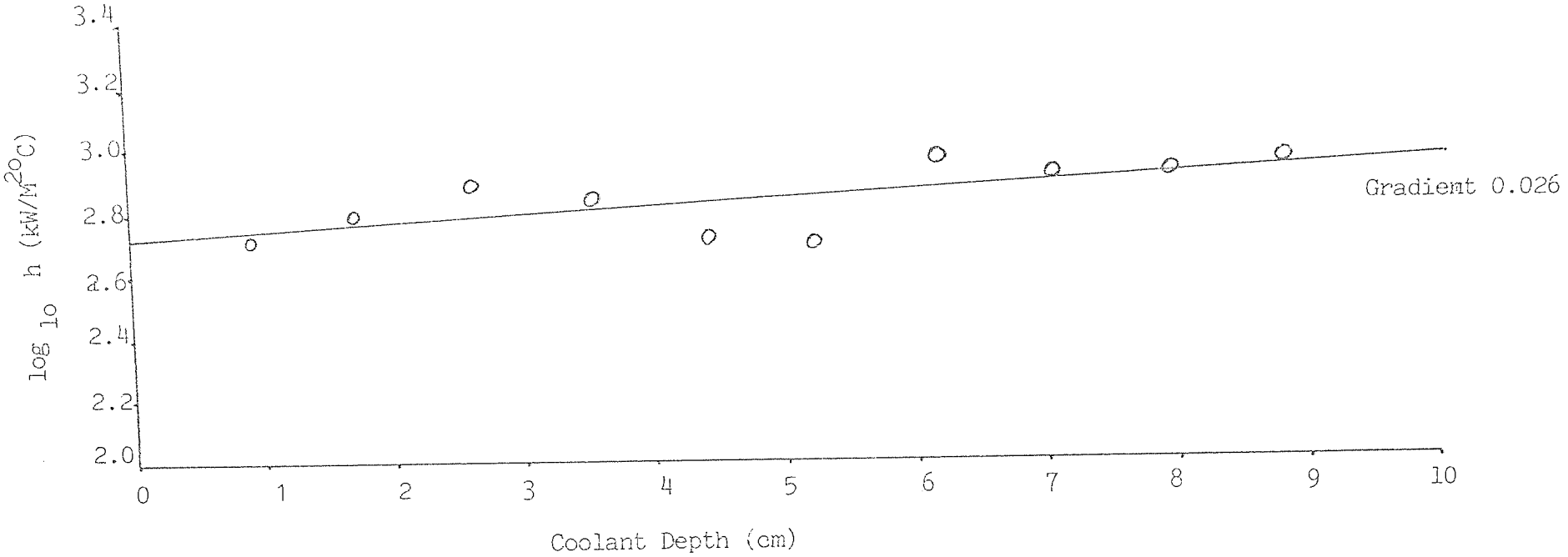

Figure 6.09 Plot of $\log_{10}$ Heat Transfer Coefficient (h) against Coolant Depth

Coolant Temperature 90°C

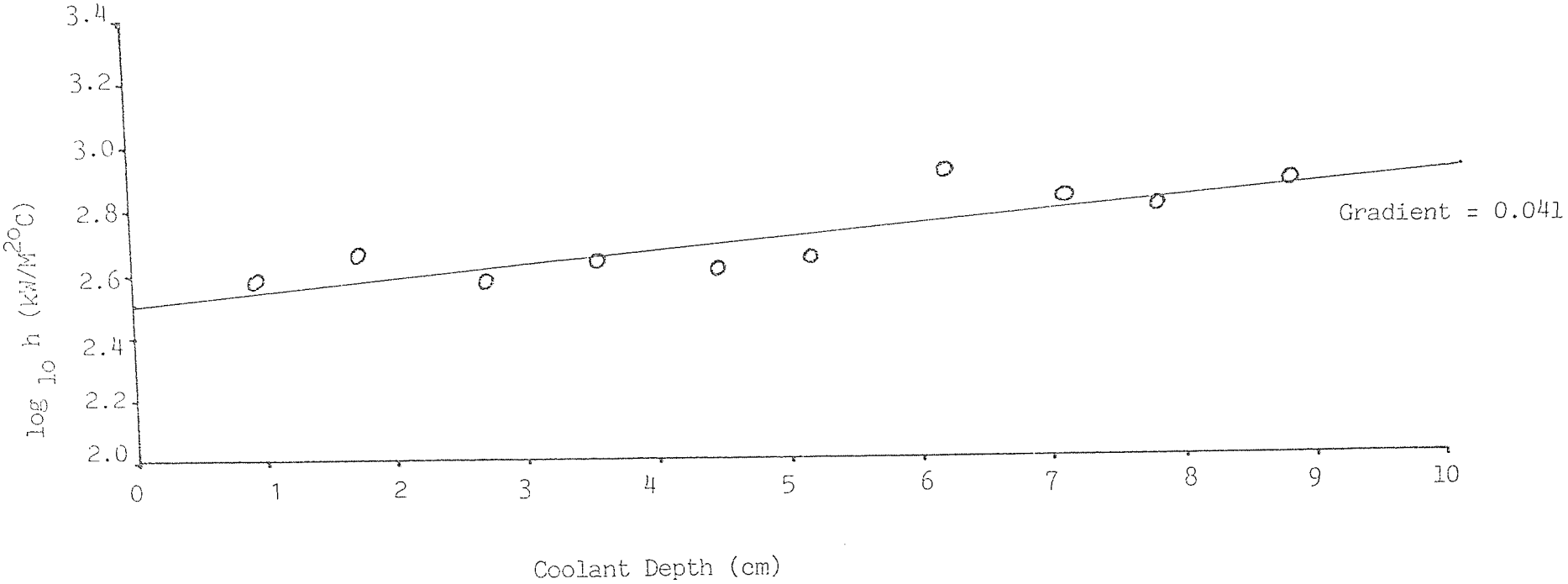

Figure 6.10 Plot of $\log_{lo}$ Heat Transfer Coefficient (h) against Coolant Depth.

Coolant Temperature $95^{o}C$.

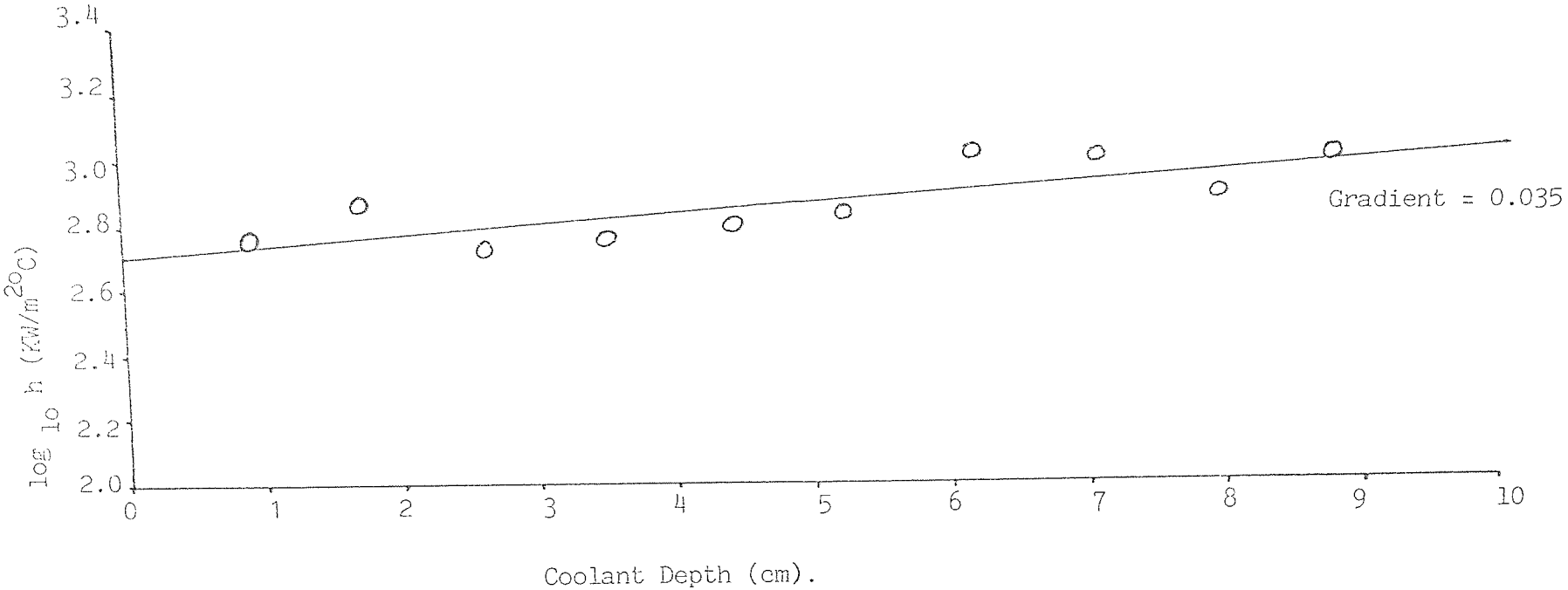

Chapter VII

Conclusions

This research has attempted to provide information on heat transfer between molten materials and liquids. This was achieved by using molten metal and water systems. In order to obtain the necessary experimental data for this study, an apparatus was successfully designed and built which enabled molten metal to be flooded with pre-heated water and the resultant temperature change in the molten metal to be measured and recorded.

A simple heat transfer model, based on fundamental heat transfer mechanisms was developed and applied to the experimentally obtained data. This enabled heat fluxes and also surface temperatures of the cooling metal to be calculated. The latter was achieved without the use of a semi-infinite solid, transient heat flow model. The experiments produced constant heat fluxes of several seconds duration and thus improved the reproduceability of the experiments by not yielding transient heat fluxes.

The experimental results were plotted as $\log_{10}$ Heat Flux against $\log_{10}\theta$, where $\theta = T_s - T_c$. This yielded a relationship which can be compared to those derived from heat flux data obtained from other heater types under saturated pool boiling conditions at atmospheric pressure. The complete classical boiling curve was not obtained due

to temperature constraints produced by the metals used for the experiments.

The heat transfer coefficient was found to be positively correlated to the depth of coolant, but not strongly related to the degree of subcooling of the coolant over the range investigated. This is to be expected as the heat transfer coefficient was calculated from the relationship

$$h = \frac{q'}{\theta} \qquad 7.01$$

and thus contains the coolant temperature. However it is well worth noting that heat transfer appears to be a function of T_s, T_c, and (T_s-T_c) the latter being the dominant function. T_s was difficult to control experimentally as it was a function of the molten metal bulk temperature and the coolant temperature and the heat transfer rate, which is a dependent variable. Heat transfer, as measured by heat flux, between molten metals and water was found to be a strong function of temperature and not a strong function of the thermal and physical properties of the metals themselves. These physical properties are summarised in table 7.01 below and can be seen to be dissimilar.

Table 7.01 - Summary of Physical Properties from reference (93)

Metal	M.P.+(^{o}C)	k(W/m^{o}C)	(Kg/m^3)	C(J/Kg^{o}C)	T_{ref} ^{o}C
Aluminium	660	98.7	2,346	1,080	800
Lead	327	18.2	10,450	137	500
Tin	232	33.4	6,897	241	400

This suggests that the results of this research can be applied to other metal/water heat transfer situations which are under similar conditions of time, temperature and pressure.

The experimental heat flux data are summarised in figure 7.01 overleaf. It can be seen that heat transfer occurred in the film boiling region, and included both the transition and stable sub-regions. Maximum heat fluxes occurred in the region of nucleate boiling crisis. This corresponded to a heat flux of 1,585 kWm^{-2} at a value of 159^{o}C. A well defined minimum heat flux region was found to occur between transition film boiling and stable film boiling. This region of minimum heat flux or Leidenfrost point was found to have a value of approximately 63.1 kWm^{-2} and corresponded to a value of 610^{o}C.

Boiling dynamics have been advanced as triggering mechanisms for fuel coolant interactions, Swift (67) has suggested nucleate boiling, and Board (68)and (69) has suggested transition film boiling.

The result of this research indicates that nucleate boiling could only be applied to low melting metals and would not be applicable to the many commercially used medium and high melting point metals. F.C.I. were not encountered in the many experiments conducted in this research, even at subcooling of 95^{o}C, i.e. water at an initial bulk temperature of 5^{o}C.

FIGURE 7.01 SUMMARY OF EXPERIMENTAL HEAT FLUX DATA

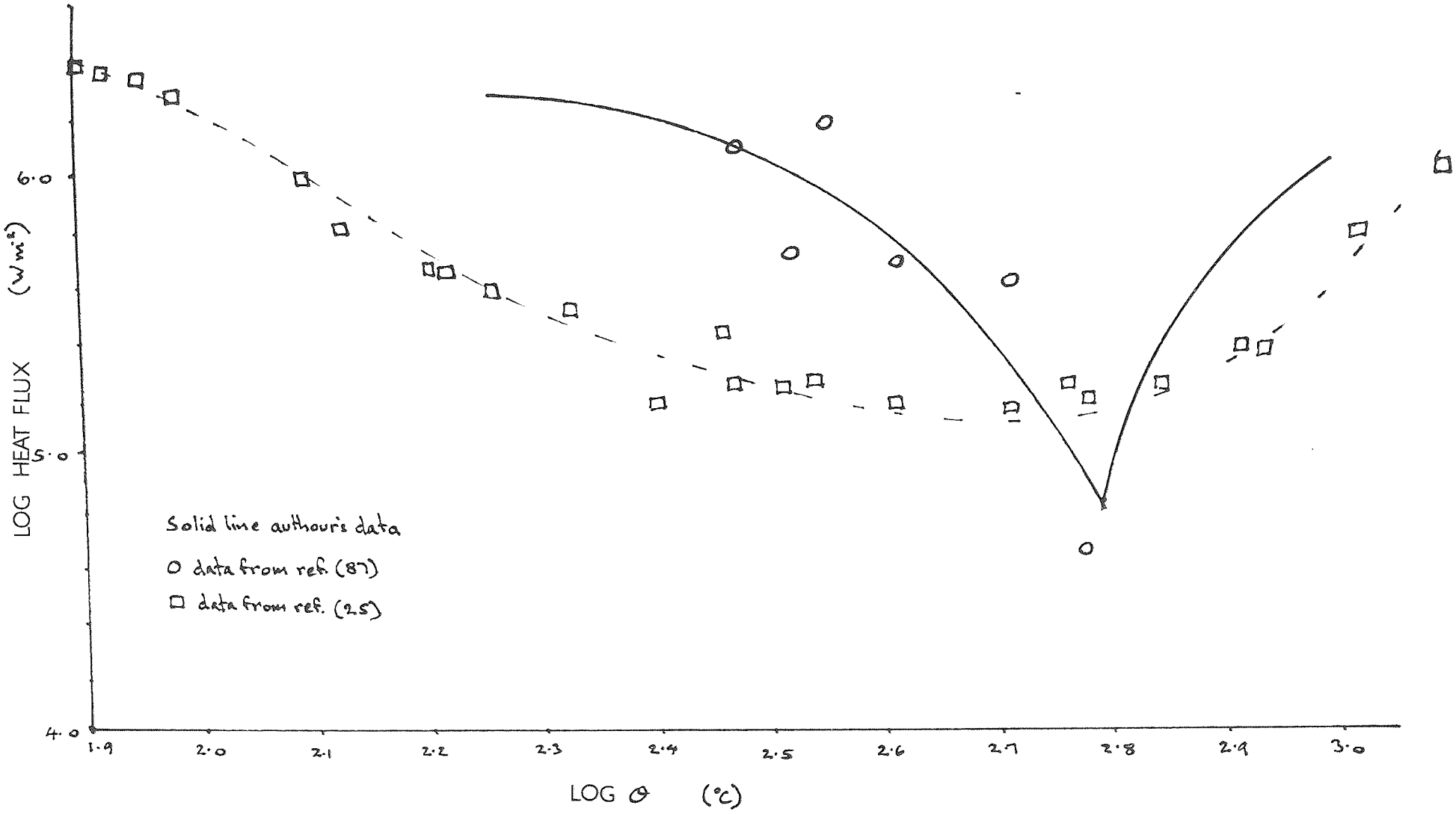

Experiments yielded typically uniform cooling rates, though at high subcooling more than one cooling mode was occasionally encountered. This produced a cooling curve with two or at most three clearly different gradients. Each such gradient was treated as an experiment and was processed as outlined in Chapter VI.

This research has produced results which indicate that when a molten metal is flooded with water so that no mixing of the hot and cold liquids occurs, heat flows from the metal to the liquid at a steady rate over a time interval of several seconds. The longest time recorded was ten seconds. This suggests that boiling dynamics did not play, in these tests, a triggering role in situations where the fuel is stationary and only essentially convective forces are acting on a non-entrapped shallow coolant.

The long time intervals and the low heat transfer rates that were found to occur around the Leidenfrost point indicate that very effective coarse mixing of a molten fuel and coolant may be caused by some external agency, without appreciable loss of thermal energy from the fuel. This situation if triggered by some mechanism would enable an energetic F.C.I. to occur.

The results indicate that molten metal and water are effectively decoupled by a vapour blanket and that it would be possible for coarsely mixed molten metal and water to separate out under the influence of gravity and for the metal to reform as a coherent mass on the base of the container.

From figure 7.01, page 73, it can be seen that the experimental results in the transition film boiling region are supported by data from Konuray (87), obtained by quenching crucibles of molten tin in water.

The results of Farber and Scorah (25) for a wire heated under water at atmospheric pressure yield similar maximum and minimum heat fluxes, though clearly show nucleate boiling to occur at lower heater temperatures. Both nucleate boiling regions fall into the temperature range of 100° to $270^{\circ}C$ obtained by Kenrick (41) for the onset of boiling in water. It is suggested that the higher heater temperature obtained for nucleate boiling is due to the heater surface being deficient in active nucleation sites, thus enabling a higher superheat to be obtained. It would be reasonable to expect a solid surface to be deficient in active nucleation sites if it had been obtained from a liquid / liquid interface between molten metal and water. The resultant surface would be highly deficient in entrapped non-condencable gases due to the nature of its formation, and therefore from the work of Cole (28) and Bankoff (44) would be expected to be deficient in active nucleation sites.

At higher heater temperatures nucleation sites become inactive due to vapour blanket formation and the differences in the heater surfase would be expected to be reduced and thus yield similar heat fluxes, for similar condions. Data trends in the film boiling region are approximately a factor of three different from each other, and are similar to the difference in the heat flux in the Leidenfrost region. The higher heat fluxes of Farber and Scorah (25) for this region may be due to still active nucleation sites on their heater surface as compared to the heaters used by Konuray (87) and the auther.

References

1. Epstein, L.F. General Electric Report, GEAP 3242, p.37 (1959).

2. Witte, L.C., Cox, J.E. and Bouvier, J.E. J.Metals, 22 (1970).

3. Dullforce, T.A., Buchanan, D.J. and Peckover, R.S. J.Phys.D. Appl. Phys., 9, p.1295. (1976).

4. Page, F.M., Private Communication (1977).

5. Page, F.M., Private Communication (1978).

6. Pamphlet in the Ironbridge Museum.

7. Morrison, E.E., 'Men, Machines and Modern Times' p.154. MIT Press (1966).

8. Macdonald, 'Volcanoes' Prentice Hall. (1973).

9. Jennings, A.J.D., 'The Physical Chemistry of Safety' The Chem. Eng. October (1974).

10. King, R. Process Engineering p.69. September (1975).

11. Hughes, J.R., 'Storage and Handling of Petroleum Liquids: Practice and Law' 2nd Ed. pp.145 and 220, Griffin (1970).

12. Burgess, D.S., Murphy, J.N., and Zabetakis, M.G., 'Hazards Associated With The Spillage of L.N.G. on Water' Report of Investigation 7448, u.s. Dept. of the Interior Bureau of Mines, November (1970).

13. Nelson, W., and Kennedy, E.H., 'What Causes Kraft Dissolving Tank Explosions, I.Laboratory Experiments'. Paper Trade Journal, Vol. 140, Part 29, pp. 50-56, July (1956).

14. Nelson, W., and Kennedy, E.H., 'What Causes Kraft Dissolving Tank Explosions, II. Mill Investigations', Paper Trade Journal, Vol. 140, Part 30, pp. 30-32, July (1956).

15. Taylor, M.L., and Gardner, H.S., 'Causes of Recovery Boiler Explosions'. TAPPI, Vol. 57, No.11, pp. 76-78, November (1974).

16. Vaughan, G.J., 'A Consideration of Some Self-Initiating Mechanisms for F.C.I.'s' CLM/RR/S2/6, August (1975).

17. Buxton, L.D., and Nelson, L.S., 'Core-Melt-Down Experimental Review, Chapt. 6, Steam Explosions SAND 74-0382, August (1975).

18. Health and Safety Executive 'The Explosion at Appleby - Frodingham Steelworks Scunthorpe, 4th November, 1975'. H.M.S.O. (1976).

19. Carslaw, H.W., and Jaeger, J.C. 'Conduction of Heat in Solids. OUP, 2nd Edition (1959).

20. Fauske, H.K., Nucl. Sci. Eng., 51. p.95 (1973).

21. Tong, L.S., 'Boiling Heat Transfer and Two-Phase Flow' p.1. John Wiley and Sons, New York. (1965).

22. Nukiyama S., 'Maximum and Minimum Valves of Heat Transmitted from Metal to Boiling Water under Atmospheric Pressure' J.Soc.Mech.Eng. Japan 37 p.367 (1934).

23. Leidenfrost, J.G., De Aquae Communis Nonnullis Qualitatibus Tractatus. Duisberg on Rhine. (1756). English transl. Wares, C., DeGolyer Collection in the History of Science and Technology, University of Oklahoma. (1963).

24. Lang, C., Trans. Int. Eng. Shipbuilders (Scotland) 32 pp. 279 - 295 (1888).

25. Farber, E.A., and Scorah, R.L., 'Heat Transfer to Water Boiling under Pressure'. Trans. ASME 70, pp.369 - 384 (1948).

26. McAdams, W.H., Woods. W.K., and Bryan, R.L., 'Vaporization inside Horizontal Tubes' Trans ASME 63 pp. 545 - 552 (1941).

27. Forster, K., and Greif, R., 'Heat Transfer to a Boiling Liquid; Mechanism and Correlations', Trans. ASME, Ser C, J. Heat Transfer 81, pp. 43 - 53 (1959).

28. Cole, R., 'Boiling Nucleation' Adv.Heat Trans. Vol. 10 pp. 85 - 166 (1974).

29. Becker,R., and Doring, W., Ann. Phys (Leipzig) 24 p.719 (1935).

30. Volmer, M., 'Kinetic der Phasenbildung' Steinkopff, Dresden-Leipzig, (1939).
English trans. 'Kinetics of Phase Formation' Ref ATI No.81935 (F.T.S.-7068-RE) Clearinghouse Fed. Sci. Tech. Inform Springfield, Virginia.

31. Frenkel, J., 'Kinetic Theory of Liquids' Dover, New York (1955).

32. Reiss, H., Ind. Eng. Chem. 44, 1284. (1952).

33. Lothe, J. and Pound, G.M., J.Chem.Phys. 36, 2080 (1962).

34. Reiss, H., Katz, J.L. and Cohen, E.R., J.Chem.Phys. 44, p.1269 (1952).

35. Hirth, J.Pound Pound, G.M., Progr.Mater.Sci. II, 1 (1963).

36. Zettlemoyer, A.C., ed. 'Nucleation' Dekker New York (1969).

37. Westwater, J.W., 'Boiling of Liquids', Adv.Chem.Eng. Vol.2 Academic Press (1958).

38. Bernath, L., Ind.Eng.Chem. 44, 1310 (1952).

39. Enger.T. and Hortman, E.E., 'LNG spillage on Water: 1 Exploratory Research on Rapid Phase Transformations' Shell Pipeline Corp. Tech. Report No. 1-71 Feb. (1971).

40. Apfel, R.E., 'Vapour Cavity Formation in Liquids', NR.384-903. Tech. Memorandum No.62, Harvard University AD 704, 593. February (1970).

41. Kenrick, F.B., Gilbert, C.S. and Wismer, K.L., J.Phys. Chem. 28, 1297 (1924).

42. Briggs, L.J. J.Appl.Phys. 26, 1001 (1955).

43. Bankoff, S.G., AlCh E.J. 4, 24 (1958).

44. Bankoff, S.G., Chem. Eng. Prog., Symp. Ser. No. 29 (Vol.55), 87 (1959).

45. Fisher, J.C., J.Appl. Phys. 19, 1062 (1948).

46. Bankoff, S.G., Trans. ASME 79, 735 (1957).

47. Apfel, R.E. J.Chem.Phys. 54, - 62 (1971).

48. Rohsenow, W. and Griffith, P., 'Correlation of Maximum Heat Transfer Data for Boiling of Saturated Liquids,' Chem.Eng.Progr. Symp. Ser.52 No. 18, 47 (1956).

49. Zuber, N., 'Hydrodynamic Aspects of Boiling Heat Transfer,' USAEC Report AECU-4439. (1959).

50. Addoms, J.N., 'Heat Transfer at High Rates to Water Boiling Outside Cylinders' D.Sc.Thesis Massachusetts Institute of Technology (1948).

51. Chang, Y.P., and Suyder, N.W., 'Heat Transfer in Saturated Boiling', Chem. Eng. Progr. Symp. Ser. 56, No.30, 25-38 (1960).

52. Kutateladze, S.S., 'Heat Transfer in Condensation and Boiling' USAEC Report AEC-tr-3770 (1952).

53. Zuber, N., Tribus, M. and Westwater, J.W., 'The Hydrodynamic Crisis in Pool Boiling of Saturated and Subcooled Liquids', International Developments in Heat Transfer, Pt II, 230-236, ASME (1961).

54. Kutateladze, S.S. and Schneiderman, L.L., 'Experimental Study of Influence of Temperature of Liquid on Change in Rate' 95-100 in 'Problems of Heat Transfer during a Change of State,' USAEC Report AEC-tr-3405 (1953).

55. Westwater, J.W. and Santangelo, J.G., 'Photographic Study of Boiling' Ind.Eng.Chem. 47, 1605-1610 (1955).

56. Bromley, L.A.,'Heat Transfer in Stable Film Boiling' Chem. Eng. Progr. 46, 221-227 (1950).

57. Berenson, P.J., 'Film-Boiling Heat Transfer From a Horizontal Surface', Journal of Heat Transfer 351-358 August (1961).

58. Vaughan, G.J., The Metal/Water Explosion Phenomenon A Review of present understanding SRD R177 May (1980).

59. Nakanishi, E. and Reid, R.C., Chem.Eng.Prog.67, 37 (1971).

60. Katz, D.L. and Sliepcevich, C.M., Hydrocarbon Processing, p.240 November (1971).

61. Henry, R.E. and Fauske, H.K., Paper presented at the Third Specialist Meeting on Sodium-Fuel Interaction in Fast Reactors, Tokyo April (1976).

62. Ochiai, M. and Bankoff, S.G., Paper presented at the International Conference on Fast Reactor Safety and Related Physics, Chicago, October (1976).

63. Long, G., 'Explosions of Molten Aluminium in Water- Cause and Prevention' Metal Progress 71 (5) 107-112 (1957).

64. Hess, P.D. and Brondyke K.J., 'Causes of Molten Aluminium - Water Explosions' Metal Progress 95, (4) 93-100 (1969).

65. Page, F.M., 'Base Triggered F.C.I. in Copper/Water Systems Paper presented at 4th CSNI Specialist Meeting on Fuel-Coolant Interaction in Nuclear Reactor Safety April (1979).

66. Buchanan, D.J. and Dullforce, T.A. Nature, 245, 34 (1973).

67. Swift, D., Argonne National Laboratory, Chemical Engineering Division Semi-Annual Report, 192, ANL-7125 Jul-Dec (1965).

68. Board, S.J., et al., 'An Experimental Study of Energy Transfer Processes Relevant to Thermal Explosions' Int. Journal of Heat and Mass Transfer 14 (10) 1631-1641 (1971).

69. Board, S.J., Farmer, C.L. and Poole, D.H., 'Fragmentation in Thermal Explosions,' Int.Journal of Heat and Mass Transfer, 17 (2) 331-339 (1974).

70. Kazimi, M.S., 'Theoretical Studies of Some Aspects of the Molten Fuel-Coolant Thermal Interaction.' Report No. 31-109-39-2831 TR. MIT. MITNE-155 May (1973).

71. Stevens, J.W. and Witte, L.C., Int. J.Heat Mass Transfer 16, 669 (1973).

72. Witte, L.C., Cox, J.E. and Bouvier J.E. J.Metals 22 (1970).

73. Theofanous, T.G., Saito, M. and Efthimiadis, T., 'The Role of Hydrodynamic Fragmentation in Fuel Coolant Interactions. Paper presented at 4th CSNI Specialist Meeting on Fuel-Coolant Interaction in Nuclear Reactor Safety April (1979).

74. Bains, M., Hydrodynamic Fragmentation in a Dense Dispersion. Paper presented at 4th CSNI Specialist Meeting on Fuel-Coolant Interaction in Nuclear Reactor Safety April (1979).

75. Lamb, H., Hydrodynamics, p.370, 6th ed., Cambridge University Press, London (1932).

76. Zuber, N., 'On Stability of Boiling Heat Transfer', Trans. ASME, 80, 771-720 (1958).

77 Zyszkowski, W., 'Thermal Interaction of Molten Copper with Water' Int.Journal of Heat and Mass Transfer 18 (2) 271-287 (1975).

78. Zyszkowski, W., 'Study of the Thermal Explosion Phenomenon in Molten Copper-Water System', Int.Journal of Heat and Mass Transfer 19 (8) 849-867 (1976).

79. Knapp, R.B. and Todreas, N.E. Nucl. Eng. and Design 35,69 (1975).

80. Flory, K., Paoli, R. and Mesler, R.B., Chem. Eng. Prog. 65, (12) 50 (1969).

81. Epstein, M., 'A New Look at the Cause of Thermal Fragmentation' Am. Nucl. Soc. Trans., 19, (1974).

82. Epstein, M., 'Thermal Fragmentation - A gas Release Phenomena' Nucl. Soc. and Eng. 55 (1974).

83. Baker, L.A. and Ward, R.G. J.Iron and Steel Inst. 205, 714 (1967).

84. Johnson, G.W. and Shuttleworth, R., Phil. Mag. 4957 (1959).

85. Frederking, T.H.K. and Clark, J.A., 'Natural Correction Film Boiling on a Sphere'. Adv.Crys. Eng. 8, 501-506 (1962).

86. Caldarola, L. and Ladisch, R., 'Film Boiling Experiments at Karlsruke.' Paper presented at 4th CSNI Specialist Meeting on Fuel-Coolant Interactions in Nuclear Reactor Safety. April (1979).

87. Konuray, M.M.,'The Interactions of Hot Spheres and Volatile Liquids'. Ph.D.Thesis June (1975).

88. Dullforce, T.A., Private Communication (1978).

89. Nelson, L.S. and Buxton, L.D., 'The Thermal Interaction of Molten L.W.R. Core Materials with Water'. Sand. 77-0170C. Sandia Laboratories, Alburquerque. (1977).

90. Manual on the use of thermocouples in temperature measurements ASTM STP 470 (1970).

91. Miller, E.C., Ch.4 'Liquid Metals Handbook' Office of Naval Research, U.S. Government Printing Office (1955).

92. Data Lab. Technical Services, Datalab, Surrey. (1977).

93. Smithells, C.J., 'Metals Reference Book' 5th Ed. Butterworth (1976).